Accepted Manuscript

Synthesis and biological evaluation of novel 2-heteroarylimino-1,3-thiazolidin-4-ones as potential anti-tumor agents

Germain Revelant, Sophie Huber-Villaume, Sandrine Dunand, Gilbert Kirsch, Hervé Schohn, Stéphanie Hesse

PII: S0223-5234(15)00149-X

DOI: 10.1016/j.ejmech.2015.02.053

Reference: EJMECH 7735

To appear in: *European Journal of Medicinal Chemistry*

Received Date: 16 September 2014

Revised Date: 26 February 2015

Accepted Date: 27 February 2015

Please cite this article as: G. Revelant, S. Huber-Villaume, S. Dunand, G. Kirsch, H. Schohn, S. Hesse, Synthesis and biological evaluation of novel 2-heteroarylimino-1,3-thiazolidin-4-ones as potential anti-tumor agents, *European Journal of Medicinal Chemistry* (2015), doi: 10.1016/j.ejmech.2015.02.053.

Graphical abstract

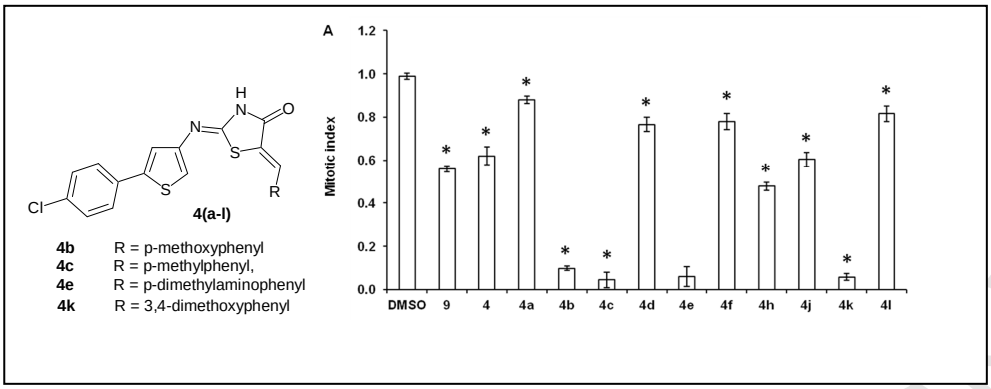

Synthesis and biological evaluation of novel 2-heteroarylimino-1,3-thiazolidin-4-ones as potential anti-tumor agents

Germain Revelant[1,a], Sophie Huber-Villaume[2,b], Sandrine Dunand[1], Gilbert Kirsch[1], Hervé Schohn[2,] ** and Stéphanie Hesse[1,] *

1. Université de Lorraine - UMR CNRS 7565 - Structure et Réactivité des Systèmes Moléculaires Complexes – Equipe 3 (HECRIN) - 1 Boulevard Arago, 57070 Metz Technopôle, France
2. Université de Lorraine - UMR CNRS 7565 - Structure et Réactivité des Systèmes Moléculaires Complexes – Equipe 5 (2MIC) – Campus Bridoux – rue du Général Delestraint – 57070 Metz Cedex, France

*Corresponding author: Tel.: +33 3 87 54 74 97. Fax: + 33 3 87 31 58 01.
** Corresponding author: Tel.: +33 3 87 37 84 09. Fax:+ 33 3 87 31 58 01
E-mail addresses: herve.schohn@univ-lorraine.fr (H. Schohn), stephanie.hesse@univ-lorraine.fr (S. Hesse)

a and b, Authors contributed equally to this article

Keywords : thiazolidinone, thiophene, thiazole, antiproliferative activity, colon cancer

Abstract

A series of 35 heteroarylimino-1,3-thiazolidinones with three sites of functionalization were synthesized and their antiproliferative properties were studied. The *in vitro* screening by MTT assay was performed against five cancer cell lines (human colon cancer cell lines HT29, HCT116 and SW620 and breast cancer cell lines MCF7 and MDA-MB-231). It was observed that N3-substituted thiazolidinones had moderate activities whereas 5-benzylidene thiazolidinones showed promising activities. To investigate the mechanism of action, detailed biological studies of six selected compounds (those presenting the lower mitotic index) were carried out on the human colon cancer HT29 cell line. Cell cycle assay revealed that those compounds induced cell accumulation in G2/M and in subG0/G1 phases of cell cycle. Moreover, dissipation of mitochondria membrane potential was observed as well as redox changes in treated cells.

1. Introduction

Colon cancer is one of the most frequent cancer diseases in the world. Most popular anti-cancer drugs belong to molecule groups which interfere with the progression of tumour cell through cell cycle progression by limiting DNA synthesis or DNA damage reparation. In addition, another group of drugs consists in the inhibition either of the formation of mitotic spindle or in protein function, especially protein activity, involved in these mechanisms [1]. Other strategies consist in the development of chemotherapeutic drugs which inhibit G2/M transition concomitantly with apoptosis cell death, such as thiazolidinone derivatives [2].
Thiazolidinone moiety belongs to an important family of heterocyclic scaffold presenting diverse biological activities such as antimicrobial [3], antidiabetic [4] or anticonvulsant [5]. This scaffold has attracted continuing interest over the years [6-7]. Especially, 2-imino-4-thiazolidinones have also been investigated for their pharmacological properties. For example, darbufelone has showed anti-inflammatory activity [8], whereas 2-heteroarylimino-1,3-thiazolidin-4-ones, especially thiazolylimino- and benzothiazolylimino- derivatives, were described as antifungal or antibacterial compounds [9, 10]. 5-Benzylidene-2-phenylimino-1,3-thiazolidin-4-ones **I** were reported for their anticancer activity [11] and a complete SAR study was realized on their anti-tumour activity against non-small cell lung cancer cell line H460 and its paclitaxel-resistant variant $H460_{taxR}$ (Fig. 1) [12]. 2-Phenylimino-5-(3-methoxybenzylidene)-3-propyl-1,3-thiazolidin-4-one **II** was proved to induce cell growth arrest after human colon adenocarcinoma-derived HT29 cells exposure for 72h (IC_{50} = 64.1µM) [13]. Recently thiazolidin-4-ones **III** substituted with indolin-2-one fragment were evaluated against four human cancer cells as HT29, human gastric H460, mammary adenocarcinoma-derived MDA-MB-231 and sarcoma-derived SMMC-7721 cells, and the compounds showed promising antiproliferative activity [14].

Novel 2-(heteroarylimino)-1,3-thiazolidin-4-ones **IV** with three different sites of functionalization were synthesized and tested for their antiproliferative effect against human colon and breast cancer–derived cells by MTT assay. Based on this first screening, several molecules were selected to investigate their mechanism of action. Especially, cell cycle distribution, induction of apoptosis and redox changes were studied.

2. Results and discussion

2.1. Chemistry

A first series of six 2-[5-aryl-3-thienyl]imino-1,3-thiazolidin-4-ones **1-6** were synthesized according to the synthetic pathway described in Scheme 1. 3-Aminothiophenes were reacted with chloroacetyl chloride and then with ammonium thiocyanate [15]. A second series of

compounds **4(a-l)** were synthesized starting from **4,** the most active compound of the first series. For this purpose, derivative **4** was condensed with several aldehydes in presence of pyrrolidine in methanol (Scheme 1 and Supporting Information S1.1).

To test effect of nitrogen N3 substitution on antiproliferative activity, the synthesis of a third series of compounds was carried out using two different pathways highlighted in Scheme 2. Firstly, 3-aminothiophenes were converted into the corresponding isothiocyanates. Those compounds were then either condensed with p-anisidine to give the corresponding thioureas which were reacted with ethyl chloroacetate and cyclized to led compounds **7-11** (steps b and c in Scheme 2) [16] or isothiocyanates were condensed with chloroacetamides in basic media to allow formation of compounds **12-17** (step d in Scheme 2 and Supporting Information S1.2).

Finally, variation was made on heteroarylimino moiety. Derivatives **18-19** were synthesized starting from 3-aminoselenophene [17] and aminothiazole. Those thiazolidinones were then modified by introducing substituents on position 5 to give derivatives **20-24** (Scheme 3 and Supporting Information S1.3).

2.2. Biological results

2.2.1. In-vitro cytotoxicity

Using the MTT method, antiproliferative activity of synthesized compounds was evaluated against human colon cancer cell lines (HT29, HCT116 and SW620) and breast cancer cells (MCF7 and MDA-MB-231). Among compounds **1-6** (Table 1), compound **4** inhibited HT29 cell growth with an IC_{50} estimated at 17.1 ± 7.2 µM but had however no effect on the other cell lines used (IC_{50}> 50µM). It should also be noted that compound **18,** selenophene analogue of compound **4**, displayed no cytotoxicity whatever the cell line tested (Table 1) whereas compound **19**, thiazole analogue of compound **4**, showed moderate anticancer activity against HT29 and HCT116 cells (IC_{50} values estimated at 8.9 ± 2.1 µM and 23.8 ± 6.8 µM, respectively).

Derivatives **4 (a-l),** obtained starting from **4,** presented diverse subtitutions at 5-position of the thiazolidine ring (Scheme 2 and Table 1). With exception of derivatives **4g** and **4i** (bearing respectively 4-hydroxybenzylidene and heptylidene), all those compounds were more potent than **4** (IC_{50}< 12 µM on HT29 cells). 4-Methoxybenzylidene (**4b**), 4-methylbenzylidene (**4c**), 4-chlorobenzylidene (**4d**), 4-dimethylaminobenzylidene (**4e**), 4-bromobenzylidene (**4f**), 2-naphtylidene (**4h**) and 4-fluorobenzylidene (**4l**) substitutions gave the higher cell growth inhibitory effect. Similar results were obtained when the experiments were performed with the other cell lines with some exceptions: SW620 cell exposure to compounds **4b** and **4h** led to IC_{50} estimated at 28.1 ± 12.4 and > 50 µM, respectively. A similar IC_{50} was calculated when

HT29 (11.5 ± 7.0 µM) or MDA-MB-231cells (10.9 ± 0.5 µM) were treated with compound **4j**, but higher IC_{50}values were obtained when the other cell lines were tested.

Compounds **7-17** presenting diverse substitutions on N3 of the thiazolidinone ring were also evaluated (Scheme 2 and Table 1). With the exception of compound **9,** the synthesized derivatives were less efficient to alter colorectal or mammary cell growth than compounds **4(a-l)**.

Finally, derivatives **20-24**, synthesized starting from **19**, were evaluated for their respective cytotoxicity (Scheme 3 and Table 1). IC_{50} values were at the micromolar range after cell exposure to compounds **20-22.** Similar results were obtained when cells were exposed to compound **23**, with the exception of SW620 cells (IC_{50} = 20.3 ± 2.8 µM). In addition, treatment with compound **24** was efficient to inhibit HT29 and HCT116 cell growth, but it had no effect when the other cell lines were used. IC_{50} values were however greater than those obtained for compounds **20-22** (Table 1).

Collectively, compounds **4**(**a-l**) and **20–23** reduced colorectal cell growth. Some of those compounds were selected to further investigate mechanisms of HT29 cell death.

2.2.2. Cell cycle assay

To confirm results obtained by MTT procedure, HT29 cells were treated with each compound at concentration corresponding to IC_{50} value over three days with daily medium changes. Cells were counted by the Trypan blue method. In these conditions, cell growth inhibition reached 90 % when cells were exposed to compounds **4b**, **4c**, **4e** or **4k** (Fig. 2A). Lower inhibitions were obtained with compound **4d** (25%), **4f** (25%), **4h** (50%), **4j** (40%), **4l** (25%) or **9** (50%). However, when HT29 cells were treated with compounds **20-23** at concentration corresponding to IC_{50} value, cell growth inhibition was less than 25% (Fig. 2B). HT29 cells were therefore treated with 1-10 µM of each compound (Fig. 2B). In these experimental cell culture conditions, cell growth inhibition reached 90 %, when HT29 cells were exposed to 2.5 µM of compound **20** or **22**. Growth inhibition was estimated at 40% after cell exposure to 10µM of compound **21** (Fig. 2B). When cells were treated with compound **23**, less than 5 % cell growth inhibition was observed whatever the concentration tested (not shown).

Cell growth kinetic curves were further established and HT29 cell viability was tested by flow cytometry after treatment with compound **4b**, **4c**, **4e** or **4k** over three days (Fig. 3A). Each compound altered dramatically cell growth and levels of living cells decreased concomitantly (Fig. 3B). Similar results were obtained after treatment with 2.5 µM of compound **20** or **22** (Fig. 3C and 3D) but the effect on cell viability was lower as compared to the results obtained with compound **4** derivatives suggesting that those compounds had rather a cytostatic impact on HT29 growth.

Cell distribution in cell cycle phases after cell exposure to each compound was analyzed. Cell accumulation in G2/M phase was found after cell exposure to compound **4b**, **4c**, **4e** or **4k** (Table 2). When HT29 cells were treated with compound **20** or **22**, cells accumulated slightly in G2/M phase. Interestedly, cell exposure to compound **4b**, **4c**, **4e**, **4k**, **20** or **22** involved cell accumulations in sub-G1 fraction, supporting that each treatment triggered cells to apoptosis cell death (Table 2). Moreover, it was observed by the use of DAPI probe loaded on treated cell layers that chromatin condensation and nuclear fragmentation occurred in treated cells (Supporting Information S2). Cell death was associated also with the loss of mitochondrial membrane potential (ψ_m) as demonstrated by the absence of J-aggregates when HT29 cells were exposed to each compound together with JC-1 fluorescent probe (Supporting Information S2).

Since IC_{50} was near or less than 10 µM (Table 1), impact of compounds **4a**, **4f, 4j** and **9** was also studied (Fig. 2A). In brief, whatever the molecule tested, cell exposure to each compound was not associated to cell accumulation in sub-G1 fraction. Cell treatment with compound **4a**, **4f** or **4j** increased cell distribution in S-phase of cell cycle whereas cells accumulated slightly in G0/G1 after exposure to compound **9**. Collectively, those results suggested that molecule treatment was associated rather to cytostatic cell growth arrest.

2.2.3. Changes in redox statut

Oxidative stress is related to the induction of autophagy, the cell defence against cell injury. Ultimately, activation of autophagy process is linked to cell death in association or not with apoptosis [18, 19]. As oxidative stress induces apoptosis [20], ROS and RNS levels were quantified in cells exposed to thiazolidin-4-one derivatives **4b**, **4c**, **4e**, **4k**, **20** or **22.**

Fluorescent probe DCF-2DA was used to quantify any change in ROS levels after cell exposure to thiazolidin-4-one derivatives over 6 hours (Fig. 4). ROS levels reached a peak one hour after compound **4b** treatment (Fig. 4A). ROS levels increased with the maximum reached at 4 hours and they decreased over 6 hours to ROS content found in DMSO-treated cells. A similar situation was obtained when cells were exposed to compound **4k**; but ROS levels reached a peak 30 min after drug treatment. Compound **4e** treatment increased gradually ROS production and reached maximum at 4 hours; ROS levels decreased slightly thereafter. It was similar to that obtained when HT29 cells were treated with compound **4c**. Similar ROS production curve was observed when cells were exposed to compound **20**. ROS levels reached a peak at 3 hours whereas compound **22** did not alter ROS content within the cells over 6 hours-treatment duration (Fig. 4B).

DAF-2DA detects reactive oxygen- and nitrogen-derived species and notably nitric oxide. DHR123 probe is used to detect peroxynitryl radical. As shown in table 3 and with the exception of compound **22**, each compound treatment involved the production of RNS species detected by DAF-2DA probe. In addition slight but significant decreases of peroxynitryl

radical levels were obtained when cells were treated with compound **4b**, **4c**, **4e, 4k** or **22**, whereas peroxynitryl content increased after cell exposure to compound **20** (Table 3).

Since thiazolidin-4-one derivative treatment induced the production of reactive species with the exception of compound **22,** the cytoplasmic GSH content was quantified as it is often depleted in the presence of an excess of reactive species (Table 3). GSH content was decreased up to 30 % when cells were exposed to compound **4c** whereas 10-15%-GSH decreases were obtained after cell exposure to compounds **4b** and **4e**. In contrast, there was no significant change in GSH levels in cell homogenates treated with compound **4k** or **20**. Finally, pre-treatment with ascorbic acid, an antioxidant, protected cells against stress injury but it did not rescue HT29 cell growth (Table 4) supporting that the oxidative stress observed was not solely involved in cell death observed.

Moreover, generation of reactive species could activate the NF-2E related factor 2/Kelch like-ECH-associated protein 1 (Nrf2/Keap1) pathway, involved to protect cells against oxidative stress [21]. Activation of the Nrf2/Keap1 pathway leads to the stabilization of Nrf2 which translocates in nuclei and binds to Maf protein. The complex, after binding to specific DNA sequence, defined as antioxidant response element localised in the promoter of Nfr2/Maf target genes, increases the transcription of genes involved in reactive species-mediated response such as Heme Oxygen-1 (HO-1), NADH quinone oxidase-1 (NQO1) or glutamyl-cysteyl ligase (GCL). As shown in figures 4C and 4D, HT 29 treatment with derivatives **4c** and **4d** did not induced HO-1 expression. In contrast, NQO-1 and GCL expression were increased supporting that other pathways could regulate the expression of the enzymes as described previously [22, 23]. However, the increases of GCL expression, which is the rate-limiting enzyme in the synthesis of GSH, correlated well with the decreases of GSH levels observed when cells were treated with thiazolidin-4-one derivatives **4c** and **4e** (Table 3 and Fig. 4C). Similarly, cell exposure to derivative **4k** did not affect GSH content and GCL expression stayed constant (Table 3 and Fig. 4D). Finally, the distribution of Nrf2 protein by cell fractionation was also studied. However, Nfr2 protein levels were not increased in nuclei homogenates prepared from treated cells over 6 hours. Similar results *id est* absence of Nrf2 translocation and no increase of HO-1, NQO-1 or GCL respective expression, were obtained when HT29 cells were treated with compounds **4b**, **4e**, **20** and **22** (Supporting Information S3 and S4).

2.2.4. Autophagy detection

As cell growth arrest and redox changes in treated cells have been observed, autophagy detection was realized. As shown in figure 5A, acidic vesicles contents were increased within HT29 treated cells over two days, as demonstrated by the use of acridine orange dye. Moreover, beclin-1 expression, a marker of autophagosome formation, was induced after cell exposure to each molecule (Fig. 5B). Thus, our results supported that HT29 exposure to

thiazolidin-4-one derivatives was associated with autophagy process. However, it could not be concluded whether autophagy process results in HT29 cell apoptosis cell death or whether compound treatment is associated to autophagy cell death as previously discussed [24].

3. Conclusions

35 Thiazolidinone derivatives were tested for their antiproliferative activity against a panel of five cancer cell lines. It was shown that substitution with an aryl group on N3 of thiazolidinone ring reduced dramatically the anti-cancer activity whereas substitution by a benzylidene group on position 5 is really important. Especially, it was found that compounds with a p-methoxybenzylidene (**4b**), p-methylbenzylidene (**4c**), p-dimethylaminobenzylidene (**4e**) and 3,4-dimethoxybenzylidene (**4k**) enhanced the impact on HT29 cell growth arrest. For these compounds, cell underwent apoptosis cell death after cell accumulation in G2/M phase of the cell cycle, as described previously with another thiazolidinone derivative. On the other hand, it was demonstrated that cell exposure to the selected compound was associated with the production of reactive species, and the induction of autophagy which could lead to cell death [24]. Of note, increasing the production of reactive species represents also an alternative among the chemotherapeutic strategies against cancer cells (for review, [25]). Therefore, further studies are needed to decipher cell death mechanism involved in HT29 cell exposed to the selected thiazolidin-4-one derivatives.

4. Experimental

4.1. Chemistry

All solvents were of reagent grade and, when necessary, were purified and dried by standard methods. All chemicals were purchased from Acros or Sigma-Aldrich. All reactions were routinely checked by TLC analysis on an Alugram SIL G/UV_{254} (Macherey-Nagel) with spots visualized by UV light. The concentration of solutions after reactions and extractions involved the use of a rotary evaporator operating at reduced pressure. Organic solutions were dried over anhydrous magnesium sulfate, and column chromatography was performed using silica gel 60 (50-200 µm diameter). Melting points were determined in open capillaries on a Stuart SMP3 apparatus and are uncorrected. The ^{1}H and ^{13}C NMR spectra were measured on an AC Bruker 250 MHz spectrometer in $CDCl_3$ or DMSO-d_6; chemical shifts are reported in parts per million (ppm). All coupling constants (*J*) are given in Hz. MS spectra were recorded on an Agilent Technologies GC-MS instrument equipped with a 7683 injector, 6890N gas chromatograph and a 5973 mass selective detector. The mass spectrometer was operated in EI mode at 70 eV, and MS spectra were recorded from m/z 50 to 650. Elemental analyses (C, H, N, S) were used to confirm the purity of all compounds (>95%) and were performed on a CHN ThermoScientific Flash 2000 apparatus.

Thienyliminothiazolidinones **1-6** and their N-methoxyphenyl derivatives **7-11** were obtained via already reported procedures respectively [15] and [16].

4.1.1. General method for the functionalization of 5-position of the thiazolidinone. Access to compounds **4(a-l)** and **20-24**

Thiazolidinone **4** or **19** (0.5 mmol) was dissolved in methanol (20 mL) and pyrrolidine (0.5 mmol) was added. The corresponding aldehyde (0.5 mmol) was added under stirring and the mixture was refluxed overnight. After cooling to room temperature, the precipitating product was filtered, washed with methanol (10 mL) and diethyl ether (10 mL), and dried.

It must be noted that ^{13}C NMR of some following products can not be performed due to their low solubility.

*4.1.2. 2-{[5-(4-Chlorophenyl)-3-thienyl]imino}-5-benzylidene-1,3-thiazolidin-4-one (**4a**)*

Yellow solid ; yield : 56% ; mp 269°C ; ^1H NMR (DMSO-d_6) δ_H7.18 (s, 1 H, CH), 7.40 (s, 1 H, CH), 7.45-7.78 (m, 10 H, 10 × CH), 12.11 (s, 1 H, NH); ^{13}C NMR (DMSO-d_6) δ_C 112.8, 118.3, 121.1, 126.8, 129.1, 129.2, 129.6, 129.8, 130.6, 131.9, 132.2, 132.4, 133.3, 133.8, 141.1, 141.8; HRMS (ESI) : *m/z* calcd for $[C_{20}H_{13}ClN_2OS_2 + H]^+$: 397.0231 ; found : 397.0256.

*4.1.3. 2-{[5-(4-Chlorophenyl)-3-thienyl]imino}-5-(4-methoxybenzylidene)-1,3-thiazolidin-4-one (**4b**)*

Yellow solid ; yield : 75% ; mp 285°C ; ^1H NMR (DMSO-d_6) δ_H 3.77 (s, 3 H, OCH_3), 7.03-7.16 (m, 3 H, 3 × CH), 7.39-7.77 (m, 8 H, 8 × CH) , 12.17 (s, 1 H, NH); ^{13}C NMR (DMSO-d_6) δ_C 55.3, 114.8, 120.9, 126.8, 126.9, 129.1, 129.2, 129.7, 130.9, 131.5, 131.7, 131.9, 132.2, 132.4, 132.6, 141.8, 160.6; HRMS (ESI) : *m/z* calcd for $[C_{21}H_{15}ClN_2O_2S_2 + H]^+$: 427.0336 ; found : 427.0354.

*4.1.4. 2-{[5-(4-Chlorophenyl)-3-thienyl]imino}-5-(4-methylbenzylidene)-1,3-thiazolidin-4-one (**4c**)*

Yellow solid ; yield : 69% ; mp 284°C ; ^1H NMR (DMSO-d_6) δ_H2.31 (s, 3 H, CH_3), 7.17 (s, 1 H, CH), 7.27-7.52 (m, 7 H, 7 × CH), 7.58-7.77 (m, 3 H, 3 × CH) , 12.26 (s, 1 H, NH); HRMS (ESI) : *m/z* calcd for $[C_{21}H_{15}ClN_2OS_2 + H]^+$: 411.0387 ; found : 411.0402.

*4.1.5. 2-{[5-(4-Chlorophenyl)-3-thienyl]imino}-5-(4-chlorobenzylidene)-1,3-thiazolidin-4-one (**4d**)*

Pale Brown solid ; yield : 71% ; mp 282°C ; ^1H NMR (DMSO-d_6) δ_H7.16 (s, 1 H, CH), 7.39-7.77 (m, 10 H, 10 × CH) , 12.27 (s, 1 H, NH); HRMS (ESI) : *m/z* calcd for $[C_{20}H_{12}Cl_2N_2OS_2 + H]^+$: 430.9841 ; found : 430.9844.

*4.1.6. 2-{[5-(4-Chlorophenyl)-3-thienyl]imino}-5-(4-dimethylaminobenzylidene)-1,3-thiazolidin-4-one (**4e**)*

Orange solid ; yield : 79% ; mp 288°C ; ^1H NMR (DMSO-d_6) δ_H 2.96 (s, 6 H, 2 × CH_3), 6.75-6.84 (m, 2 H, 2 × CH), 7.15 (s, 1 H, CH), 7.36-7.71 (m, 8 H, 8 × CH) , 12.02 (s, 1 H, NH); HRMS (ESI) : *m/z* calcd for $[C_{22}H_{18}ClN_3OS_2 + H]^+$: 440.0653 ; found : 440.0655.

*4.1.7. 2-{[5-(4-Chlorophenyl)-3-thienyl]imino}-5-(4-bromobenzylidene)-1,3-thiazolidin-4-one (**4f**)*

Green solid ; yield : 68% ; mp 298°C ; ^1H NMR (DMSO-d_6) δ_H7.16 (s, 1 H, CH), 7.39 (s, 1 H, CH), 7.45-7.77 (m, 9 H, 9 × CH), 12.33 (s, 1 H, NH); HRMS (ESI) : *m/z* calcd for $[C_{20}H_{12}BrClN_2OS_2 + H]^+$: 476.9315 ; found : 476.9322.

*4.1.8. 2-{[5-(4-Chlorophenyl)-3-thienyl]imino}-5-(4-hydroxybenzylidene)-1,3-thiazolidin-4-one (**4g**)*

Green solid ; yield : 76% ; mp 253°C ; ^{1}H NMR (DMSO-d_6) δ_H6.84-6.92 (m, 2 H, 2 × CH), 7.13 (s, 1 H, CH), 7.38-7.70 (m, 8 H, 8 × CH) , 12.33 (s, 1 H, NH); ^{13}C NMR (DMSO-d_6) δ_C 112.4, 116.2, 118.8, 121.0, 124.2, 124.6, 126.8, 129.1, 130.1, 131.8, 132.0, 132.2, 132.4, 141.0, 141.7, 159.3; HRMS (ESI) : *m/z* calcd for $[C_{20}H_{13}ClN_2O_2S_2 + H]^+$: 413.0180 ; found : 413.0218.

*4.1.9. 2-{[5-(4-Chlorophenyl)-3-thienyl]imino}-5-(2-naphtylidene)-1,3-thiazolidin-4-one (**4h**)*

Yellow solid ; yield : 89% ; mp 288°C ; ^{1}H NMR (DMSO-d_6) δ_H7.21 (s, 1 H, CH), 7.41-8.17 (m, 13 H, 13 × CH) , 12.29 (s, 1 H, NH), ^{13}C NMR (DMSO-d_6) δ_C 112.2, 112.8, 118.1, 120.8, 124.1, 126.7, 126.8, 128.1, 128.3, 129.1, 129.2, 129.3, 131.1, 131.3, 131.8, 132.1, 132.2, 132.4, 132.7, 134.4, 141.1, 141.9; HRMS (ESI) : *m/z* cald for $[C_{24}H_{15}ClN_2OS_2 + H]^+$: 447.0387 ; found : 447.0385.

*4.1.10. 2-{[5-(4-Chlorophenyl)-3-thienyl]imino}-5-heptylidene-1,3-thiazolidin-4-one (**4i**)*

Brown solid ; yield : 60% ; mp 191°C ; ^{1}H NMR (DMSO-d_6) δ_H0.78-0.84 (m, 3 H, CH_3), 1.22-1.39 (m, 8 H, 4 × CH_2), 2.10-2.14 (m, 2 H, CH_2), 6.70-6.73 (m, 1 H, CH), 7.07 (s, 1 H, CH), 7.34 (s, 1 H, CH), 7.44-7.52 (m, 2 H, 2 × CH), 7.63-7.71 (m, 2 H, 2 × CH), 12.05 (s, 1H, NH); ^{13}C NMR (DMSO-d_6) δ_C 13.9, 21.9, 27.3, 28.3, 30.9, 32.5, 112.4, 118.2, 120.9, 126.7, 129.1, 131.9, 132.2, 132.3, 132.5, 134.6, 141.0, 141.6; HRMS (ESI) : *m/z* calcd for $[C_{20}H_{21}ClN_2OS_2 + H]^+$: 405.0857 ; found : 405.0859.

*4.1.11. 2-{[5-(4-Chlorophenyl)-3-thienyl]imino}-5-(2-pyridylmethylene)-1,3-thiazolidin-4-one (**4j**)*

Orange solid ; yield : 76% ; mp 291°C ; ^{1}H NMR (DMSO-d_6) δ_H7.11 (s, 1 H, CH), 7.31-7.50 (m, 3 H, 3 × CH), 7.59-7.92 (m, 5 H, 5 × CH), 8.67-8.75 (m, 2 H, 2 × CH), 12.19 (s, 1 H, NH); ^{13}C NMR (DMSO-d_6) δ_C 112.7, 118.3, 121.0, 123.4, 123.6, 126.7, 126.9, 127.3, 129.1, 132.3, 137.3, 137.4, 141.0, 141.7, 149.2, 151.5, 151.6; HRMS (ESI) : *m/z* cald for $[C_{19}H_{12}ClN_3OS_2 + H]^+$: 398.0183 ; found : 398.0179.

*4.1.12. 2-{[5-(4-Chlorophenyl)-3-thienyl]imino}-5-(3,4-dimethoxybenzylidene)-1,3-thiazolidin-4-one (**4k**)*

Yellow solid ; yield : 72% ; mp 242°C ; ^{1}H NMR (DMSO-d_6) δ_H3.77 (s, 3 H, OCH_3), 3.82 (s, 3 H, OCH_3), 7.10-7.21 (m, 4 H, 4 × CH), 7.41-7.48 (m, 2 H, 2 × CH), 7.57-7.68 (m, 4 H, 4 × CH), 12.18 (s, 1 H, NH); HRMS (ESI) : *m/z* calcd for $[C_{22}H_{17}ClN_2O_3S_2 + H]^+$: 457.0442 ; found : 457.0442.

*4.1.13. 2-{[5-(4-Chlorophenyl)-3-thienyl]imino}-5-(4-fluorobenzylidene)-1,3-thiazolidin-4-one (**4l**)*

Orange solid ; yield : 54% ; mp 223°C ; ^{1}H NMR (DMSO-d_6) δ_H7.18 (s, 1 H, CH), 7.30-7.51 (m, 5 H, 5 × CH), 7.60-7.77 (m, 5 H, 5 × CH) , 12.21 (s, 1 H, NH); ^{13}C NMR (DMSO-d_6) δ_C 116.2, 116.6, 121.0, 126.8, 126.9, 129.1, 129.2, 130.1, 130.5, 132.0, 132.1, 132.2, 132.4, 132.6, 141.1, 141.8; HRMS (ESI) : *m/z* cald for $[C_{20}H_{12}ClFN_2OS_2 + H]^+$: 415.0136 ; found : 415.0160.

*4.1.14. 2-{[4-(4-Chlorophenyl)-1,3-thiazol-2-yl]imino}-5-(4-dimethylaminobenzylidene)-1,3-thiazolidin-4-one (**20**)*

Orange solid ; yield : 86% ; mp> 300°C ; ^{1}H NMR (DMSO-d_6) δ_H3.05 (s, 6 H, 2 × CH_3), 6.89 (d, 2 H, 2 × CH, *J*= 8.75Hz), 7.51-7.62 (m, 5 H, 5 × CH), 8.01 (d, 2 H, 2 × CH, *J*=8.75Hz), 7.93 (s, 1 H, CH), 12.51 (s, 1 H, NH); HRMS (ESI) : *m/z* calcd for $[C_{21}H_9ClN_4OS_2 + H]^+$: 441.0605 ; found : 441.0615.

*4.1.15. 2-{[4-(4-Chlorophenyl)-1,3-thiazol-2-yl]imino}-5-(4-methylbenzylidene)-1,3-thiazolidin-4-one (**21**)*

Yellow solid ; yield : 68% ; mp> 300°C ; ^{1}H NMR (DMSO-d_6) δ_H2.38 (s, 3 H, CH_3), 7.40 (d, 2 H, 2 × CH, *J*= 8.25Hz), 7.53-7.58 (m, 4 H, 4 × CH), 7.66 (s, 1 H, CH), 7.93 (s, 1 H, CH), 7.97 (d, 2 H, 2 × CH, *J*=8.25Hz), 12.68 (s, 1 H, NH); HRMS (ESI) : *m/z* calcd for $[C_{20}H_{14}ClN_3OS_2 + H]^+$: 412.0340 ; found : 412.0348.

*4.1.16. 2-{[4-(4-Chlorophenyl)-1,3-thiazol-2-yl]imino}-5-(4-methoxybenzylidene)-1,3-thiazolidin-4-one (**22**)*

Yellow solid ; yield : 79% ; mp> 300°C ; ^{1}H NMR (DMSO-d_6) δ_H3.86 (s, 3 H, OCH_3), 7.20 (d, 2 H, 2 × CH, *J*= 8.5Hz), 7.59-7.71 (m, 5 H, 5 × CH), 7.97 (s, 1 H, CH), 8.01 (d, 2 H, 2 × CH, *J*=8.5Hz) ,12.74 (s, 1 H, NH);HRMS (ESI) : *m/z* calcd for $[C_{20}H_{14}ClN_3O_2S_2 + H]^+$: 428.0289 ; found : 428.0290.

***4.1.17.** 2-{[4-(4-Chlorophenyl)-1,3-thiazol-2-yl]imino}-5-(2-naphtylidene)-1,3-thiazolidin-4-one (**23**)*

Yellow solid ; yield : 85% ; mp> 300°C ; ^{1}H NMR (DMSO-d_6) δ_H7.53-7.65 (m, 4 H, 4 × CH), 7.79 (d, 1 H, CH, *J*=9Hz), 7.88 (s, 1 H, CH), 7.98-8.05 (m, 5 H, 5 × CH), 8.14 (d, 1 H, CH, *J*=9Hz), 8.29 (s, 1 H, CH), 12.79 (s, 1 H, NH); HRMS (ESI) : *m/z* calcd for $[C_{23}H_{14}ClN_3OS_2 + H]^+$: 440.0340 ; found : 440.0346

*4.1.18. 2-{[4-(4-Chlorophenyl)-1,3-thiazol-2-yl]imino}-5-(4-fluorobenzylidene-1,3-thiazolidin-4-one (**24**)*

Yellow solid ; yield : 82% ; mp> 300°C ; ^{1}H NMR (DMSO-d_6) δ_H7.46-7.53 (m, 2 H, 2 × CH), 7.60 (d, 2 H, 2 × CH, *J*=8.5Hz), 7.73-7.79 (m, 3 H, 3 × CH), 7.96 (s, 1 H, CH), 7.98 (d, 2 H, 2 × CH, *J*=8.5Hz), 12.79 (s, 1 H, NH); HRMS (ESI) : *m/z* calcd for $[C_{19}H_{11}ClFN_3OS_2 + H]^+$: 416.0089 ; found : 416.0096.

*4.1.19. General procedure for the synthesis of N-substituted thiazolidinones **12-17***

To a mixture of the corresponding chloroacetamide (0.5 mmol) and potassium carbonate (0.75 mmol) in acetonitrile (5 mL) was added portionwise the corresponding isothiocyanate (0.5 mmol). The mixture was then heated at 40°C overnight. After cooling to room temperature, the mixture was poured into cold water (25 mL) and extracted with ethyl acetate. The organic layer was dried with magnesium sulfate, filtered and evaporated under reduced pressure. The expected product was purified using silica gel chromatography (Eluent : Cyclohexane/Ethyl acetate 3/1).

*4.1.20. 3-(4-Chlorophenyl)-2-{[5-(4-chlorophenyl)-3-thienyl]imino}-1,3-thiazolidin-4-one (**12**)*

Pale brown solid ; yield : 71% ; mp 80°C ; ^{1}H NMR ($CDCl_3$) δ_H 4.03 (s, 2 H, CH_2), 6.75 (d, 1 H, CH, *J*=1.5Hz), 7.01 (d, 1 H, CH, *J*=1.5Hz), 7.29-7.34 (m, 4 H, 4 × CH), 7.45-7.50 (m, 4 H, 4 × CH); ^{13}C NMR ($CDCl_3$) δ_C 32.9, 110.9, 120.1, 126.7, 129.1, 129.4, 129.6, 132.6, 133.0, 133.6, 134.9, 142.7, 146.6, 155.2, 171.0; HRMS (ESI) : *m/z* calcd for $[C_{19}H_{12}Cl_2N_2OS_2 + H]^+$: 418.9841 ; found : 418.9835.

*4.1.21. 3-Phenyl-2-{[5-(4-chlorophenyl)-3-thienyl]imino}-1,3-thiazolidin-4-one (**13**)*

Pink solid ; yield : 83% ; mp 152°C ; ^{1}H NMR ($CDCl_3$) δ_H4.05 (s, 2 H, CH_2), 6.75 (d, 1 H, CH, *J*=1.5Hz), 7.01 (d, 1 H, CH, *J*=1.5Hz), 7.31-7.38 (m, 4 H, 4 × CH), 7.46-7.52 (m, 5 H, 5 × CH) ; ^{13}C NMR ($CDCl_3$) δ_C 41.3, 110.8, 120.3, 119.8, 126.7, 127.9, 129.0, 129.4, 132.7, 133.5, 134.7, 142.5, 146.4, 155.1, 171.3; HRMS (ESI) : *m/z* calcd for $[C_{19}H_{13}ClN_2OS_2 + H]^+$: 385.0231 ; found : 385.0234.

*4.1.22. 3-(4-Methylphenyl)-2-{[5-(4-chlorophenyl)-3-thienyl]imino}-1,3-thiazolidin-4-one (**14**)*

Brown solid ; yield : 90% ; mp 107°C ; ^{1}H NMR ($CDCl_3$) δ_H2.33 (s, 3 H, CH_3), 3.97 (s, 2 H, CH_2), 6.67 (d, 1 H, CH, *J*=1.5Hz), 6.91 (d, 1 H, CH, *J*=1.5Hz), 7.16 (d, 2 H, 2 × CH, *J*=9Hz), 7.18-7.21 (m, 4 H, 4 × CH), 7.39 (d, 2 H, 2 × CH, *J*=9Hz) ; ^{13}C NMR ($CDCl_3$) δ_C 21.3, 32.9, 110.8, 120.3, 126.7, 127.7, 129.2, 130.1, 132.0, 132.7, 133.5, 139.2, 142.4, 147.0, 155.8, 171.4; HRMS (ESI) : *m/z* calcd for $[C_{20}H_{15}ClN_2OS_2 + H]^+$: 399.0387 ; found : 399.0383.

*4.1.23. 3-(4-Dimethylaminophenyl)-2-{[5-(4-chlorophenyl)-3-thienyl]imino}-1,3-thiazolidin-4-one (**15**)*

Brown solid ; yield : 84% ; mp 123°C ; ^{1}H NMR ($CDCl_3$) δ_H3.01 (s, 6 H, 2 × CH_3), 4.01 (s, 2 H, CH_2), 6.73 (d, 1 H, CH, *J*=1.5Hz), 6.79 (d, 2 H, 2 × CH, *J*=9Hz), 7.03 (d, 1 H, CH, *J*=1.5Hz), 7.18 (d, 2 H, 2 × CH, *J*=9Hz), 7.33 (d, 2 H, 2 × CH, *J*=8.5Hz), 7.48 (d, 2 H, 2 × CH, *J*=8.5Hz) ; ^{13}C NMR ($CDCl_3$) δ_C 32.8, 40.5, 110.7, 112.6, 120.4, 126.6, 128.4, 129.0, 132.8, 133.4, 142.3, 147.3, 149.5, 150.5, 156.4, 171.8; HRMS (ESI) : *m/z* calcd for $[C_{21}H_{18}ClN_3OS_2 + H]^+$: 428.0653 ; found : 428.0655.

*4.1.24. 3-(3,4-Dimethoxyphenyl)-2-{[5-(4-chlorophenyl)-3-thienyl]imino}-1,3-thiazolidin-4-one (**16**)*

Pale brown solid ; yield : 59% ; mp 181°C ; ^{1}H NMR ($CDCl_3$) δ_H3.90 (s, 3 H, OCH_3), 3.91 (s, 3 H, OCH_3), 4.02 (s, 2 H, CH_2), 6.75 (d, 1 H, CH, *J*=1.5Hz), 6.83 (d, 1 H, CH, *J*=2Hz), 6.92 (Dd, 1 H, CH, *J*=8.5Hz, *J*=2Hz), 6.95 (d, 1 H, CH, *J*=8.5Hz), 7.01 (d, 1 H, CH, *J*=1.5Hz), 7.32 (d, 2 H, 2 × CH, *J*=8Hz), 7.47 (d, 2 H, 2 × CH, *J*=8Hz) ; ^{13}C NMR ($CDCl_3$) δ_C 32.9, 56.0, 110.9, 111.2, 111.3, 120.3, 120.4, 126.7, 127.3, 129.0, 132.7, 133.5, 142.5, 147.0, 150.0, 155.9, 171.5; HRMS (ESI) : *m/z* calcd for $[C_{21}H_{17}ClN_2O_3S_2 + H]^+$: 445.0442 ; found : 445.0427.

*4.1.25. 3-(1-Naphtyl)-2-{[5-(4-chlorophenyl)-3-thienyl]imino}-1,3-thiazolidin-4-one (**17**)*

Yellow solid ; yield : 92% ; mp 98°C ; ^{1}H NMR ($CDCl_3$) δ_H 4.10 (s, 2 H, CH_2), 6.65 (d, 1 H, CH, *J*=2Hz), 7.22 (d, 1 H, CH, *J*=2Hz), 7.22 (d, 2 H, 2 × CH, *J*=8.5Hz), 7.36 (d, 2 H, 2 × CH, *J*=8.5Hz), 7.40–7.58 (m, 4 H, 4 × CH), 7.85–7.93 (m, 3 H, 3 × CH) ; ^{13}C NMR ($CDCl_3$) δ_C

33.2, 110.8, 120.3, 121.9, 125.6, 126.6, 126.7, 126.9, 127.3, 128.8, 129.0, 129.5, 130.2, 131.5, 132.6, 133.4, 134.6, 142.4, 146.9, 155.3, 171.4; HRMS (ESI) : *m/z* calcd for $[C_{23}H_{15}ClN_2OS_2 + H]^+$: 435.0387 ; found : 435.0376

*4.1.26. General procedure for the synthesis of heteroaryliminothiazolidinones **18-19** starting from aminoheterocycle*

To a solution of the corresponding heteroarylamine (10 mmol) in dry DMF (10 mL) was added dropwise chloroacetyl chloride (11 mmol) and the mixture was stirred at room temperature for 2h. The mixture was then poured into cold water (50 mL) and the formed precipitate was filtered, washed with water (2 × 10 mL) and dried.

The obtained chloroacetamide (5 mmol) was then dissolved in ethanol (20 mL) and ammonium thiocyanate was added (10 mmol). The mixture was refluxed for 3h and stirred at room temperature overnight. The precipitating product was filtered, washed with water (10 mL) and petroleum ether (10 mL), and dried.

4.1.27.** 2-{[5-(4-Chlorophenyl)-3-selenophenyl]imino}-1,3-thiazolidin-4-one **(18)

Brown solid ; yield : 78% ; mp 264°C ; ^{1}H NMR (DMSO-d_6) δ_H4.00 (d, 2 H, CH_2, *J*=8.6Hz), 7.48 (m, 2 H, 2 × CH), 7.61 (m, 2 H, 2 × CH) , 7.69 (s, 1 H, CH) , 8.19 (s, 1 H, CH) 11.43 (s, 1 H, NH); ^{13}C NMR (DMSO-d_6) δ_C35.4, 116.9, 123.8, 127.1, 129.1, 132.5, 134.2, 138.1, 146.7, 177.5, 187.9; HRMS (ESI) : *m/z* calcd for $[C_{13}H_9ClN_2OSSe + H]^+$: 356.9359 ; found : 356.9354.

*4.1.28. 2-{[4-(4-chlorophenyl)-1,3-thiazol-2-yl]imino}-1,3-thiazolidin-4-one **(19)***

Pink solid ; yield : 68% ; mp> 300°C ; ^{1}H NMR (DMSO-d_6) δ_H4.03 (s, 2 H, CH_2), 7.50 (d, 2 H, 2 × CH, *J*=8Hz), 7.89 (s, 1 H, CH), 7.96 (d, 2 H, 2 × CH, *J*=8Hz), 12.14 (s, 1 H, NH); ^{13}C NMR (DMSO-d_6) δ_C 34.9, 111.2, 127.3, 128.8, 132.4, 132.8, 149.6, 163.6, 169.2, 174.1; HRMS (ESI) : *m/z* cald for $[C_{12}H_8ClN_3OS_2 + H]^+$: 309.9870 ; found : 309.9876

4.2.Biological methods

4.2.1. Cell culture

HT29 (*APC*^{mut}, *P53*^{mut}, *K-RAS*^{wt}) and HCT116 (*APC*^{wt}, *P53*^{wt}, *K-RAS*^{mut}) cell lines have been established from colon adenocarcinoma tissue and represented colon cancer cell model behaving chromosomic and microsatellite instability, respectively. SW620 cells (*APC*^{wt}, *P53*^{mut}, *K-RAS*^{mut}) were originated from a lymphoid nodule and have been characterised as metastatic cells. MCF7 cells derived from mammary adenocarcinoma tissue. MDA-MB-231 cells were isolated from pleural effusion and characterised as metastatic cells. Colon cancer cells were cultivated in Dulbecco minimum essential medium DMEM (Eurobio, Courtaboeuf, France) supplemented with 10% (v/v) heat-inactivated (30 min at 56°C) fetal calf serum (Eurobio), 50 µg/mL gentamycin (Invitrogen, Paisley, UK) and 2 mM L-Glutamine (Eurobio). Mammary cancer cell were cultivated in RPMI medium containing 10% heat-inactivated fetal calf serum, 2mM L-Glutamine and 1% Penicillin/streptomycin (Eurobio). Cells were maintained in a humidified atmosphere of 5% CO_2 at 37°C.

4.2.2. Determination of IC_{50}

IC_{50} was calculated from results obtained by the thiazolyl blue tetrazolium bromide (MTT) procedure. In brief, cancer cells were seeded in 96 well-plates at 10^4 cells/well (Dutscher, Molsheim, France). 24 hours after seeding, increasing concentrations of each compound

(range from 0.01 to 100µM) were added to each well for 72 hours at 37°C. After incubation, the medium was discarded and 100µl/well of MTT solution (0.5 mg/ml diluted in medium) were added and incubated for 2 hours. Water-insoluble MTT formazan blue crystals were finally dissolved in DMSO. Each plate was read at 570 nm. IC_{50} was calculated using GraphPad Prism (GraphPad Software, La Jolla, CA, USA). Data are expressed as IC_{50} ± S.E.M. obtained from at least two independent experiments (n = 16).

4.2.3. Cell growth kinetics

HT29 cells were seeded in 6 well-plates. 48 hours after seeding, cells were treated daily with each molecule over three days. Dilutions of each drug were performed in DMSO prior to addition in the cell medium. Control cells were treated with 0.1% (v/v) of DMSO. At the indicating time, cells were harvested by trypsination (Trypsin /EDTA solution, Eurobio). 100µl of cell suspension were mixed to an equal volume of 0.04% (v/v) Trypan blue dye solution and living cells were counted using a Malassez hematimeter under microscopy. Data are means ± S.E.M of triplicate determination from two independent experiments. Results are expressed either as mitotic index (number of compound-treated cells related to control cells treated by 0.1% (v/v) DMSO used as compound vehicle) or cells counts ($x10^5$ cells/ml, in Figure 3).

4.2.4. Cell viability assay

Cell viability assay was performed with s imultaneous double-staining procedure using 2',7' – dichlorofluorescein diacetate (DCF-DA, viable cells) and propidium iodide (PI, dead cells). Two days after seeding, HT29 cells were treated with each molecule corresponding to the concentration of IC_{50} value for various times up to 24 hours with the exception of compound **20** and **22**, tested at 2.5 µM. Cells were loaded with 50µM DCF-DA and 25 µg/mL PI during 15 min at 37°C. After incubation, cells were harvested by trypsination, washed with PBS and finally suspended in 1 ml of the same buffer. Fluorescence was measured in 30 000 cells/sample by flow cytometry (FL-1 and FL-3; FACSCalibur, BD Sciences, Le Pont de Claix, France). Data are means ± S.E.M. of triplicate determinations from two independent experiments. Results are expressed in percentage of viable cells (negative to IP, and positive to DCF-2DA) with respect to total cells/events quantified.

4.2.5. Cell cycle analysis

HT29 cells were seeded in 6 well-plates. 48 hours after seeding, cells were treated with each molecule. Cells layers were washed twice with phosphate buffer saline (PBS), harvested by trypsination and fixed in 70% (v/v) ethanol solution for 2 hours and stored at -20°C at least 1 hour. Cells were then centrifuged at 1000g for 5 min at 4°C, washed with PBS and centrifuged again. Pellets were suspended in 1 ml PBS containing 50 µg/ml propidium iodide, 20 µg/ml of RNAse A (Sigma-Aldrich France, St Quentin Fallavier, France) and 0.1 % (v/v) Triton X100 for 20 min and they were analyzed by flow cytometry (FL2-A; Calibur). Results were quantified using the CellQuest software (BD Sciences) and cell cycle distribution was analysed using Modfit sofware (Verity Software House, Topsham, Maine, USA). Results are expressed as percentage of treated HT29 cells in each cell cycle phase. Cells in sub-G1 fraction are expressed as the percentage of total cells analysed in each experiment. Data are means ± S.E.M. of triplicate determinations from three independent experiments.

4.2.6.Cell-living imaging

HT29 cells were seeded in 35mm petri dishes and treated with each compound over two days. After incubation, cell layers were fixed in 70% (v/v) ethanol solution for 5 min, rinced twice with PBS. 1 µM 4',6'-diamidino-2-phenylindol (DAPI) in PBS was added for 15 min. In parallel, similar experimental conditions were carried on with supplementation of 1 µM 5,5',6,6'-tetrachloro-1,1',3,3'-tetraethylbenzimidazolylcarbocyanine iodide (JC-1) probe diluted in DMSO. JC-1 was used to demonstrate alteration of mitochondrial membrane potential (Ψm). After compound treatment, JC-1 probe was added to the medium for 15 min at 37°C. The protonophore carbonyl cyanide m-chlorophenylhydrazone (CCCP) at 50 µM for 15 min was used in order to dissipate Ψm which can be visualized by the absence of J-aggregates under red fluorescent filter. After incubation, cell layers were washed rapidly with warmed PBS (37°C) twice. Pictures were captured under UV fluorescent microscopy (Nikon Eclipse 80i, Nikon) equipped with a digital camera (DXM1200F, Nikon). They were further processed using NIS-Element AR 2.3 software (Nikon).

4.2.7. Quantification of oxygen and nitric oxide-derived species

Two days after seeding, HT29 cells were treated with each molecule corresponding to the concentration of IC_{50} value for various times up to 24 hours with the exception of compound **20** and **22**, tested at 2.5 µM. Cells were loaded with 50µM DCF-DA during 15 min at 37°C for ROS detection, 1 µM DAF-2DA during 30 min at 37°C for RNS detection, or 25µM DHR during 20 min at 37°C for peroxynitryl radical detection. Cell exposure to 1mM tert-butyl for one hour was used as a positive ROS-induced control. After incubation, cells were harvested by trypsination, washed with PBS and finally suspended in 1 ml of the same buffer. Fluorescence was measured in 30 000 cells/sample by flow cytometry (FL-1). When used, 1mM ascorbic acid, as an antioxidant, was added one hour before drug treatment and cells were prepared as described. Results were expressed as percentage of results obtained with treated cells related to cells treated with DMSO used as compound diluent. Data are means ± S.E.M of triplicate determination from three independent experiments.

4.2.8. GSH content determination

HT29 cells were grown in 6 well-plates. 48 hours after seeding, cells were exposed to each molecule corresponding to the concentration of IC_{50} value for 24 hours. Cell layers were washed three times with ice-cold PBS. They were then scrapped with 10% (v/v) perchloric acid ice-cold solution (pH 8.0) containing 2 mM EDTA. The homogenates were centrifuged at 15 000 g for 15 min at 4°C. The supernatant were stored at -80°C until analysis. GSH content was determined by a fluorescence-based microtiter plate method [26]. Perchloric acid-precipitated proteins (pellets) were solubilized in daily made 1 N NaOH prior to protein content determination using a modification of the procedure of Lowry et al. [27]. GSH contents were calculated as nanomole of GSH/mg of protein. Results are expressed in percentage as content of intracellular GSH related to that in DMSO-treated cells (relative GSH content). Data are means ± S.E.M of triplicate determination from three independent experiments.

4.2.9. Western blotting

HT29 cells were seeded in 25 cm^2-flasks. Total protein homogenates were prepared from drug- and DMSO-treated cells as follows; cell layers were washed twice with ice cold PBS and they were scrapped with 25 mMHepes/KOH (pH 7.5) buffer containing 10 mM EDTA, 40 mMKCl, 0.5 %(v/v) Igepal (Nonidet P40), 1 mM DTT and 0.1% (v/v) protease inhibitor mixture (Sigma). Homogenates were collected and left on ice for 30 min before centrifugation at 15,000g for 30 min at 4°C. Supernatants were stored at -80°C until use. 50 µg protein from

whole cell homogenates were resolved in 10-15% SDS PAGE and they were transferred onto nitrocellulose membranes. The saturation step was performed in Tris saline buffer (50 mM Tris/HCl (pH 7.4) containing 0.15 M NaCl and 0.01 % (v/v) Tween 20), supplemented with 5% (w/v) non-fat milk or BSA. The primary antibody prepared in the same buffer was then added. Membranes were incubated overnight at 4°C. The following antibodies were used: antibody against GCL (5529-1; Epitomics), HO-1 (1922-1; Epitomics), NQO-1 (2618-1; Epitomics) and GAPDH (MAB374; Millipore). Washing steps (3 times for 5 min) were performed with Tris saline buffer. The blots were then incubated 45 min in this buffer containing the horseradish peroxidase-conjugated species-specific antibody, and finally washed 3 times for 5 min with the same buffer. Blots were developed by chemo-luminescence detection according to the manufacturer's protocol (Santa Cruz Biotech). Each blot was stripped and used to detect human GAPDH (1: 10 000) using the same protocol. Bands were quantified and normalized to GAPDH content. The ratio, level of protein of interest *versus* GAPDH content, in DMSO-treated cells was considered as 1.00. Results shown are representative of one out of three independent experiments.

4.2.10. Detection of autophagy process

HT29 cells were seeded in 6 well-plates and they were treated as described before for two days with daily medium changes. Cells were incubated with 1µg/ml acridine orange for 15 min, then harvested by trypsination and suspended in PBS before flow cytometry analysis. Fluorescence (FL-3) was measured in 30 000 cells/sample. Results were analysed using CellQuest and Cyflogic software and they are expressed in arbitrary unit related to those obtained with DMSO-treated cells. Results are means ± S.E.M. of triplicate determinations from three independent experiments. In parallel, cells were cultivated in 25 cm^2-flasks and treated. Total protein homogenates were prepared and western blots were performed, using Beclin-1 (1:500, BD Biosciences) and GAPDH antibodies, respectively, as a marker of autophagosome formation and an internal marker for protein loading.

4.2.11. Statistics

Differences between results from control and drug-treated cells were analysed by Student's t test and any difference was considered significant at $p < 0.05$.

Acknowledgments

We thank the 'Ministère de l'Enseignement Supérieur et de la Recherche' for Ph.D. grants to G.R. and S. H.-V.

References

1. E. Pasquier, S. Honore, D. Braguer, Microtubule-targeting agents in angiogenesis: where do we stand?, Drug Resist. Updat. 9 (2006) 74-86.

2. L.T. Vassilev, C. Tovar, S. Chen, D. Knezevic, X. Zhao, H. Sun, D.C. Heimbrook, L. Chen, Selective small-molecule inhibitor reveals critical mitotic functions of human CDK1, Proc. Natl Acad. Sci. USA 103 (2006) 10660-10665.

3. A. Deep, S. Jain, P.C. Sharma, S.K. Mittal, P. Phogat, M. Malhotra, Synthesis, characterization and antimicrobial evaluation of 2,5-disubstituted-4-thiazolidinone derivatives, Arabian J. Chem. 7 (2014) 287-291.

4. R. Maccari, R.M. Vitale, R. Ottana, M. Rocchiccioli, A. Marrazzo, V. Cardile, A.C.E. Graziano, P. Amodeo, U. Mura, A. DelCorso, Structure-activity reliationships and molecular modelling of new 5-arylidene-4-thiazolidinone derivatives as aldose reductase inhibitors and potential anti-inflammatory agents, Eur. J. Med. Chem. 81 (2014) 1-14.

5. A.P.G. Nikalje, A.N. Shaikh, S.I. Shaikh, F.A.K. Khan, J.N. Sangshetti, D.B. Shinde, Microwave assisted synthesis and docking study of N-(2-oxo-2(4-oxo-2-substituted thiazolidin-3-ylamino)ethyl)benzamide derivatives as anticonvulsant agents, Bioorg. Med. Chem. Lett. 24 (2014) 5558-5562.

6. A.K. Jain, A. Vaidya, V. Ravichandran, S.K. Kashaw, R.K. Agrawai, Recent developments and biological activities of thiazolidinone derivatives: a review, Bioorg. Med. Chem. 20 (2012) 3378-3395

7. A.C. Tripathi, S.J. Gupta, G.N. Fatima, P.K. Sonar, A. Vermab, S.K. Saraf, 4-thiazolidinones: the advances continue..., Eur. J. Med. Chem 72 (2014), 52-77 and references therein.

8. P.C. Unangst, D.T. Connor, W.A. Cetenko, R.J. Sorenson, C.R. Kostlan, J.C. Sircar, C.D. Wright, D.J. Schrier, R.D. Dyer, Synthesis and biological evaluation of 5-[[3,5-bis(1,1-dimethylethyl)-4-hydroxyphenyl)methylene]oxazoles, -thiazoles, and –imidazoles: novel dual 5-lipoxygenase and cyclooxygenase inhibitors with anti-inflammatory activity, J. Med. Chem. (1994) 322-328.

9. K. Omar, A. Geronikaki, P. Zoumpoulakis, C. Camoutsis, M. Sokovic, C. Ciric, J. Glamoclija, Novel 4-thiazolidinone derivatives as potential antifungal and antibacterial drugs, Bioorg. Med. Chem. 18 (2010) 426-432.

10. P. Vicini, A. Geronikaki, M. Incerti, F. Zani, J. Dearden, M. Hewitt, 2-Heteroarylimino-5-benzylidene-4-thiazolidinones analogues of 2-thiazolylimino-5-benzylidene-4-thiazolidinones with antimicrobial activity: synthesis and structure-activity relationship, Bioorg. Med. Chem. 16 (2008) 3714-3724.

11. S. Xu, W. Guo, F. Teraishi, J. Pang, K. Kaluarachchi, L. Zhang, J. Davis, F. Dong, B. Yan, B. Fang, Anticancer activity of 5-benzylidene-2-phenylimino-1,3-thiazolidin-4-one (BPT) analogs, Med. Chem. (2006) 597-605.

12. H.Y. Zhou, S.H. Wu, S.M. Zhai, A.F. Liu, Y. Sun, R.S. Li, Y. Zhang, S. Ekins, P.W. Swaan, B.L. Fang, B. Zhang, B. Yan, Design, synthesis, cytoselective toxicity, structutre-activity relationships, and pharmacophore of thiazolidinone derivatives targeting drug-resistant lung cancer cells, J. Med. Chem. 51 (2008) 1242-1251.

13. R. Ottana, S. Carotti, R. Maccari, I. Landini, G. Chiricosta, B. Caciagli, M.G. Vigorita, E. Mini, In vitro antiproliferative activity against human colon cancer cell lines of representative 4-thiazolidinones, Bioorg. Med. Chem. Lett. 15 (2005) 3930-3933.

14. S. Wang, Y. Zhao, G. Zhang, Y. Lv, N. Zhang, P. Gong, Design, synthesis and biological evaluation of novel 4-thiazolidinones containing indolin-2-one moiety as potential antitumor agent, Eur. J. Med. Chem. 46 (2011) 3509-3518.

15. I. Abdillahi, G. Revelant, Y. Datoussaid, G. Kirsch, Synthesis of novel 2-thienylimino-1,3-thiazolidin-4-ones, Synthesis (2010) 2543-2546.

16. G. Revelant, S. Hesse, G. Kirsch, Synthesis of novel N-subtituted 2-(hetero)arylimino-1,3-thiazolidin-4-ones, Synthesis (2010) 3319-3324.

17. G. Revelant, S. Hesse, G. Kirsch, Synthesis of novel 2-aminothieno[3,2-d]thiazoles and selenolo[3,2-d]thiazoles, Tetrahedron (2011) 9352-9357.

18. M. Dodson, V. Darley-Usmar, J. Zhang, Cellular metabolic and autophagic pathways: traffic control by redox signaling, Free Radic. Biol. Med. 63 (2013) 207-221.

19. Z. Liu, M.J. Lenardo, Reactive oxygen species regulate autophagy through redox-sensitive proteases, Dev. Cell 12 (2007) 484–485.

20. F. Teraishi, S. Wu, J. Sasaki, L. Zhang , W. Guo, J.J. Davis, F. Dong, B. Fang, Identification of a novel synthetic thiazolidin compound capable of inducing c-Jun NH2-terminal kinase-dependent apoptosis in human colon cancer cells, Cancer Res 65 (2005) 6380-6387.

21. S.K. Niture, J.W. Kaspar, J. Shen, A.K. Jaiswal, Nrf2 signaling and cell survival, Toxicol. Appl. Pharmacol. 244 (2010) 37-42.

22. T. Xie, A.K. Jaiswal, AP-2-mediated regulation of human NAD(P)H: quinone oxidoreductase 1 (NQO1) gene expression, Biochem Pharmacol 51 (1996) 771-778.

23. J. Wu, H. Xu, P.F. Wong, S. Xia, J. Xu, J. Dong, Icaritin attenuates cigarette smoke-mediated oxidative stress in human lung epithelial cells via activation of PI3K-AKT and Nrf2 signaling, Food Chem. Toxicol. 64 (2014) 307-313.

24. D. Trachootham, J. Alexandre, P. Huang, Targeting cancer cells by ROS-mediated mechanisms: a radical therapeutic approach?, Nat. Rev. Drug Discov. 8 (2009) 579-591.

25. M.M. Hippert, P.S. O'Toole, A. Thorburn, Autophagy in cancer: good, bad, or both? Cancer Res. 66 (2006) 9349-9351.

26. K. Lewicki, S. Marchand S, L. Matoub, J. Lulek, J. Coulon J, P. Leroy, Development of a fluorescence-based microtiter plate method for the measurement of glutathione in yeast. Talanta 70 (2006) 876-882.

27. O.H. Lowry, N.J. Rosebrough, A.L. Farr, R.J. Randall, Protein measurement with the Folin phenol reagent, J. Biol. Chem. 193 (1951) 265-275.

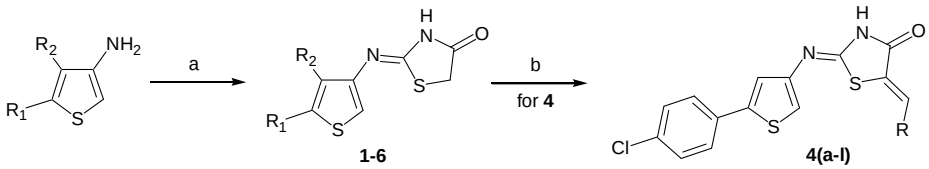

1	R_1 = p-methylphenyl, R_2 = H	**4a**	R = phenyl	**4g**	R = p-hydroxyphenyl
2	R_1 = p-methoxyphenyl, R_2 = H	**4b**	R = p-methoxyphenyl	**4h**	R = 2-naphtyl
3	R_1 = phenyl, R_2 = H	**4c**	R = p-methylphenyl,	**4i**	R = hexyl,
4	R_1 = p-chlorophenyl, R_2 = H	**4d**	R = p-chlorophenyl	**4j**	R = 2-pyridinyl
5	R_1, R_2 = naphtyl	**4e**	R = p-dimethylaminophenyl	**4k**	R = 3,4-dimethoxyphenyl
6	R_1 = tert-butyl, R_2 = H	**4f**	R = p-bromophenyl	**4l**	R = p-fluorophenyl

Scheme 1. *Reagents and conditions:* (a) i) $ClCH_2COCl$, dry DMF, rt, 2h ii) NH_4SCN, EtOH, reflux, 3h (46-90%); (b) RCHO, pyrrolidine, MeOH, reflux, 20h (56-89%).

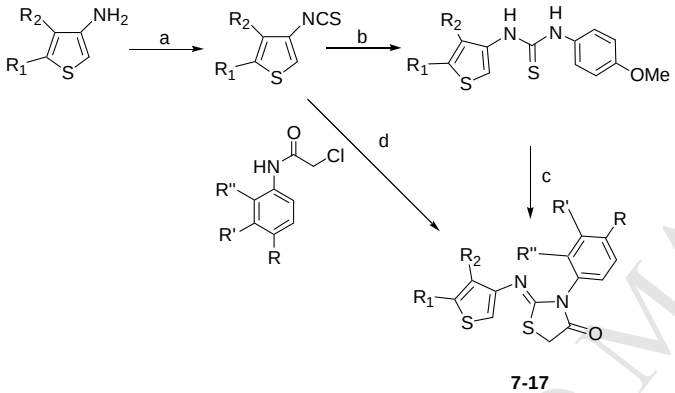

7	R_1 = Phenyl ;R_2, R', R'' = H ; R = OMe
8	R_1 = p-methylphenyl ;R_2, R', R'' = H ; R = OMe
9	R_1 = p-methoxyphenyl ;R_2, R', R'' = H ; R = OMe
10	R_1 = p-chlorophenyl ;R_2, R', R'' = H ; R = OMe
11	R_1, R_2 = dihydronaphtyl ; R', R'' = H ; R = OMe
12	R_1 = p-chlorophenyl ;R_2, R', R'' = H ; R = Cl
13	R_1 = p-chlorophenyl ;R_2, R, R', R'' = H
14	R_1 = p-chlorophenyl ;R_2, R', R'' = H ; R = Me
15	R_1 = p-chlorophenyl ;R_2, R', R'' = H ; R = NMe_2
16	R_1 = p-chlorophenyl ;R_2, R'' = H ; R, R' = OMe
17	R_1 = p-chlorophenyl ;R_2, R = H ; R', R'' = C_4H_4

Scheme 2. *Reagents and conditions:* (a) $CSCl_2$, $NaHCO_3$, $CHCl_3$, r t, 2h; (b) p-anisidine, dry CH_2Cl_2, r t, 18h; (c) $ClCH_2COOEt$, NaOAc, dry DMF, reflux, 24h; (d) K_2CO_3, CH_3CN, 40°C.

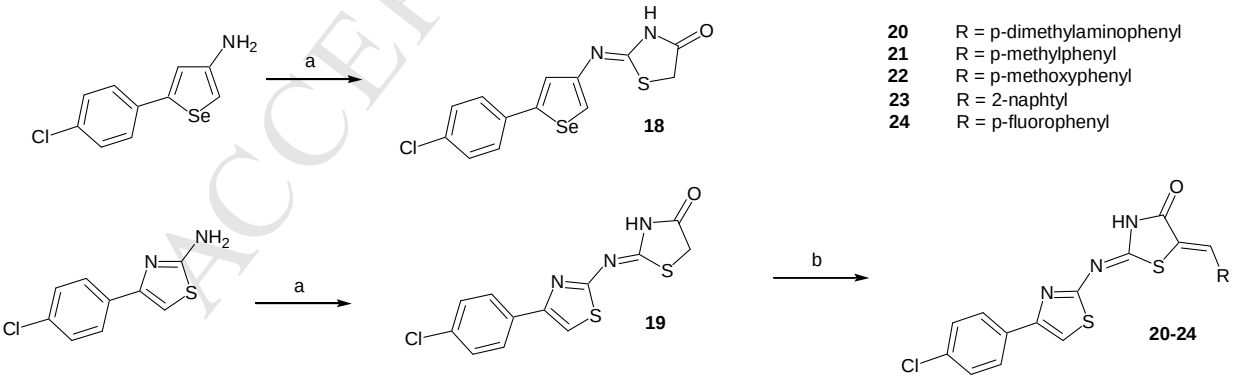

20	R = p-dimethylaminophenyl
21	R = p-methylphenyl
22	R = p-methoxyphenyl
23	R = 2-naphtyl
24	R = p-fluorophenyl

Scheme 3. *Reagents and conditions:* (a) i) $ClCH_2COCl$, dry DMF, rt, 2h ii) NH_4SCN, EtOH, reflux, 3h; (b) RCHO, pyrrolidine, MeOH, reflux, 20h.

Table 1: IC_{50} determination for thiazolidin-4-one derivatives

Compound	IC_{50} (µM)				
	HT29	HCT116	SW620	MCF7	MDA-MB-231
1	>50	>50	>50	>50	>50
2	>50	>50	>50	>50	>50
3	>50	>50	>50	>50	>50
4	17.1 ± 7.2	>50	>50	>50	>50
5	>50	>50	>50	>50	>50
6	>50	>50	>50	>50	>50
4a	10.5 ± 5.8	11.2 ± 2.2	>50	> 50	18.0 ± 0
4b	3.8 ± 0.9	1.3 ± 0.1	28.1 ± 12.4	1.0 ± 0.1	1.2 ± 0.2
4c	6.4 ± 1.5	1.0 ± 0.1	1.5 ± 0.1	0.9 ± 0.1	0.9 ± 0.04
4d	2.8 ± 2.0	11.6 ± 3.4	4.6 ± 0.7	6.7 ± 0.3	6.4 ± 0.3
4e	1.5 ± 1.2	0.5 ± 0.1	0.8 ± 0.1	0.4 ± 0.05	0.8 ± 0.01
4f	2.0 ± 1.5	3.3 ± 0.1	0.7 ± 0.6	2.5 ± 0.3	3.5 ± 0.2
4g	>50	ND	ND	> 50	ND
4h	3.7 ± 3.1	3.0 ± 0.6	>50	1.2 ± 0.1	1.8 ± 0.1
4i	33.5 ± 4.4	ND	ND	> 50	ND
4j	11.5 ± 7.0	21.6 ± 1.1	>50	30.2 ± 6.5	10.9 ± 0.5
4k	10.9 ± 3.1	1.7 ± 0.2	>50	7.6 ± 0.7	1.9 ± 0.1
4l	4.1 ± 0.6	7.4 ± 0.7	8.7 ± 1.6	> 50	ND
7	38.3 ± 7.7	ND	ND	ND	ND
8	> 50	41.0 ± 9.0	> 50	>50	>50
9	11.7 ± 1.1	2.7 ± 0.05	3.5 ± 0.1	1.9 ± 0.4	2.7 ± 0.2
10	24.6 ± 7.8	> 50	33.0 ± 6.6	> 50	> 50
11	> 50	ND	ND	> 50	ND
12	36.6 ± 3.9	ND	> 50	>50	ND
13	41.4 ± 7.4	ND	ND	> 50	ND
14	28.9 ± 8.6	ND	>50	> 50	ND
15	29.2 ± 4.3	ND	ND	> 50	ND
16	14.1 ± 2.7	49.8 ± 11.9	> 50	18.7 ± 2.6	46.9 ± 4.8
17	> 50	ND	19.5 ± 1.7	> 50	ND
18	> 50	ND	>50	> 50	ND
19	8.9 ± 2.1	23.8 ± 6.8	>50	> 50	> 50
20	0.5 ± 0.1	0.2 ± 0.02	0.20 ± 0.1	0.1 ± 0.02	0.3 ± 0.01
21	0.5 ± 0.2	0.5 ± 0.1	0.89 ± 0.1	0.4 ± 0.05	0.8 ± 0.1
22	0.4 ± 0.1	0.4 ± 0.03	0.05 ± 0.03	0.1 ± 0.02	0.3 ± 0.3
23	1.8 ± 0.3	1.2 ± 0.03	20.3 ± 2.8	0.3 ± 0.1	0.9 ± 0.05
24	2.9 ± 0.7	7.5 ± 4.3	> 50	>50	> 50

Viability was assessed by the MTT procedure as described in the biological methods section. IC_{50}Values are means ± S.E.M. ND ; not determined

Table 2: Cell cycle distribution after cell exposure to thiazolidin-4-one derivatives

Treatment[a]	Sub G1 fraction[b]	G0/G1 phase[c]	S phase[c]	G2/M phase[c]
DMSO (0.1%)	6.9 ± 0.5	46.1 ± 0.4	23.9 ± 0.3	30.0 ± 2.0
4b	21.6 ± 2.4*	1.2 ± 0.4#	18.2 ± 1.6#	80.6 ± 1.2#
4c	21.5 ± 1.8*	1.2 ± 0.2#	14.8 ± 2.0#	84.0 ± 1.8#
4e	29.0 ± 1.9*	1.5 ± 0.2#	14.8 ± 0.7#	83.7 ± 0.7#
4k	20.6 ± 2.2*	2.3 ± 0.9#	11.3 ± 0.9#	86.4 ± 0.6#
DMSO (0.1%)	2.3 ± 0.1	67.7 ± 0.5	21.1 ± 1.5	11.3 ± 1.0
20	16.2 ± 0.7*	60.6 ± 0.1#	20.7 ± 1.0	18.7 ± 0.7#
22	20.9 ± 1.4*	58.7 ± 0.4#	17.2 ± 1.3#	24.1 ± 1.4#

a, HT29 cells were treated with each compound as described in the biological methods section. **b**, results are expressed as percentage of cells in the sub-G1 fraction related to total cells analysed. **c**, results are expressed as percentage of cells in each phase of cell cycle. * and #, significant statistical difference ($P < 0.05$) at Student's t test; comparison between HT29-treated cells with respect to cells exposed to DMSO.

Table 3: Redox changes within HT29 cells exposed to thiazolidin-4-one derivatives

Treatment	RNS content		GSH content
	DAF-2DA	DHR 123	
0.1% (v/v) DMSO	100.0 ± 1.0	100.0 ± 4.2	100.0 ± 2.0
4b	169.7 ± 3.6*	85.9 ± 3.2*	88.8 ± 4.1*
4c	155.0 ± 0.3*	95.0 ± 3.2*	73.9 ± 8.3*
4e	294.4 ± 8.6*	80.1 ± 2.3*	84.6 ± 3.7*
4k	116.3 ± 1.1*	83.6 ± 4.9*	108.1 ± 7.9*
0.1% (v/v) DMSO	100.0 ± 1.0	100.0 ± 0.5	100.0 ± 10.5
20	144.4 ± 10.9*	157.6 ± 4.6*	109.1 ± 5.2
22	103.3 ± 1.7	80.9 ± 0.7*	117.0 ± 4.8

RNS and GSH levels were quantified as described in the biological methods section. *, significant statistical result ($P < 0.05$) at Student's t test; comparison between HT29-treated cells with respect to cells exposed to DMSO.

Table 4: Impact of thiazolidin-4-one derivatives on HT29 cells pre-treated with antioxidant.

	ROS content		Mitotic index	
	Compound alone	+ 1mM ascorbic acid*	Compound alone	+ 1mM ascorbic acid
0.1% (v/v) DMSO	100.0 ± 3.5	65.7 ± 4.7	1.00 ± 0.08	1.12 ± 0.03
4b	123.1 ± 0.3	97.0 ± 3.1	0.03 ± 0.01	0.03 ± 0.02
4c	172.0 ± 5.5	102.5 ± 4.8	0.02 ± 0.01	0.02 ± 0.01
4e	177.8 ± 1.6	133.6 ± 4.8	0.02 ± 0.01	0.02 ± 0.01
4k	141.6 ± 2.6	112.1 ± 3.9	0.04 ± 0.01	0.04 ± 0.01
0.1% (v/v) DMSO	100.0 ± 5.6	64.7 ± 2.6	1.00 ± 0.07	1.08 ± 0.04
20	252.5 ± 14.5	158.8 ± 8.5	0.13 ± 0.02	0.09 ± 0.02

ROS levels and mitotic index were calculated as described in the biological methods section. *, significant statistical result ($P < 0.05$) at Student's t test; comparison between HT29 cells pre-treated with ascorbic acid before addition of each compound with respect to cells exposed to each compound alone.

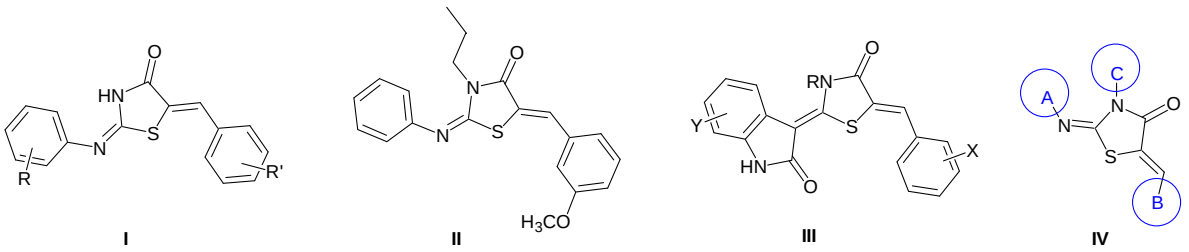

Fig. 1. Thiazolidinones described for their pharmacological activities (**I-III**) and target compounds **IV.**

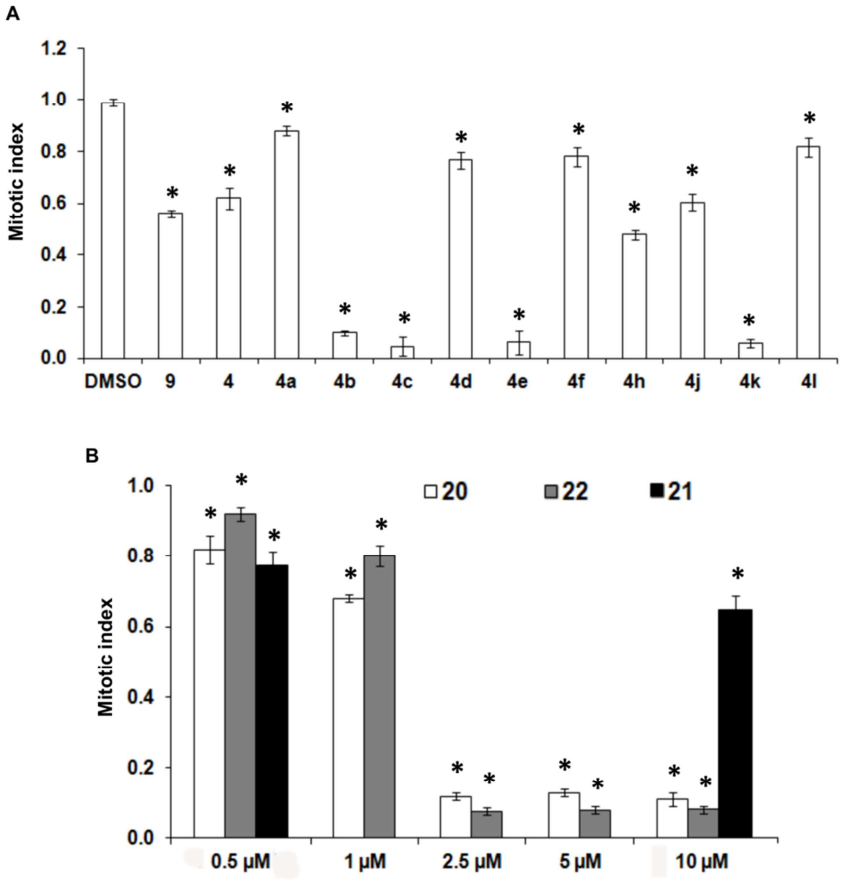

Fig. 2. HT29 cell growth inhibition of compound **4** and its derivatives.

HT29 cells were grown with compounds **4**, **4(a-l)**, and **9** (**A**) at the concentration corresponding to IC_{50} value, and with 0.5-10 µM with compounds **20** and **22** (**B**) for 72 hours. Results are expressed as mitotic index (number of compound-treated cells related to control cells treated by 0.1% (v/v) DMSO used as compound vehicle)

*, significant difference ($p<0.05$) at Student's t test between HT29-treated cells with respect to control cells, exposed to DMSO used as compound vehicle.

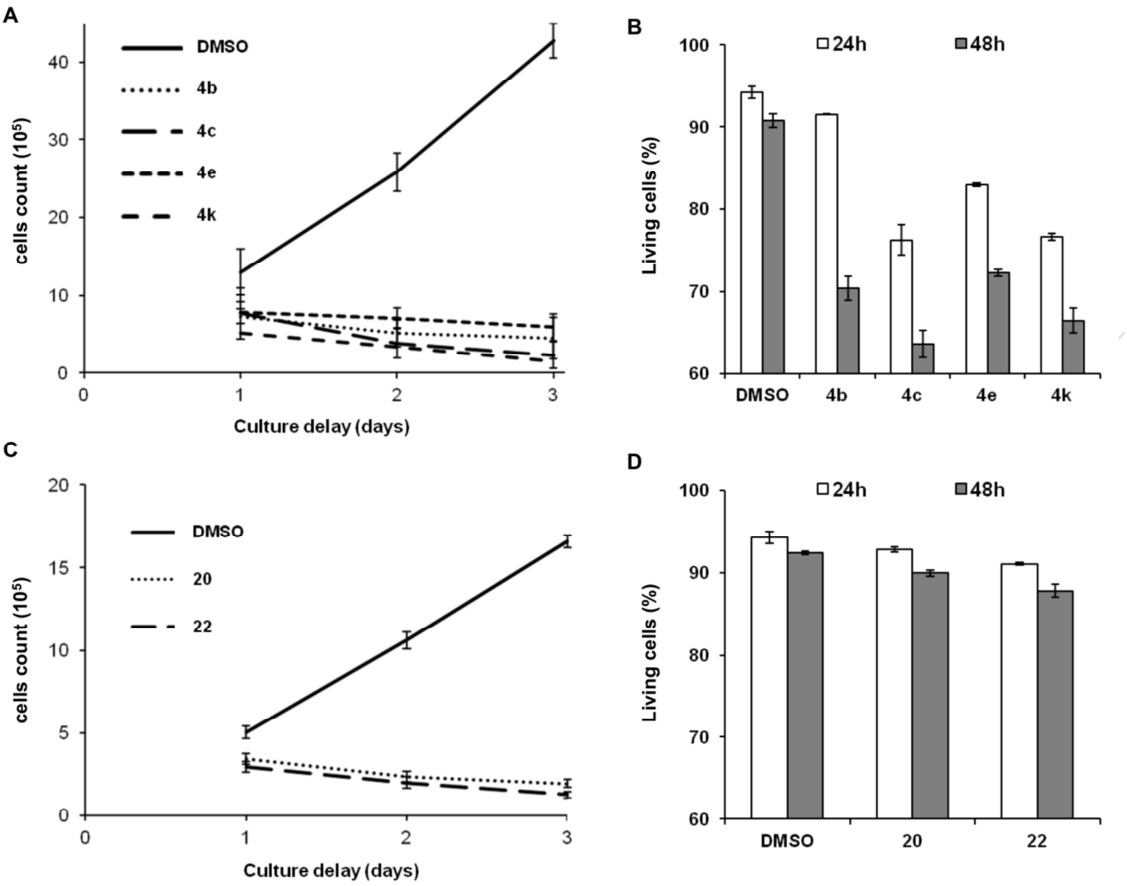

Fig. 3. HT29 cell growth kinetic and cell viability after cell exposure to compounds **4b**, **4c**, **4e**, **4k**, **20** and **22.**

Kinetic growth (**A** and **C**) and cell viability assays (**B** and **D**) were performed as described in the biological methods section. HT29 cells treated with compound **4b**, **4c**, **4e**, **4k** at the concentration corresponding to IC_{50} value (**A** and **B**) and with 2.5 µM of compound **20** and **22** (**C** and **D**). Statistical analysis demonstrated that significant difference ($P < 0.05$) at Student's t test was obtained in **A-D** (comparison between HT29-treated cells with respect to cells exposed to DMSO).

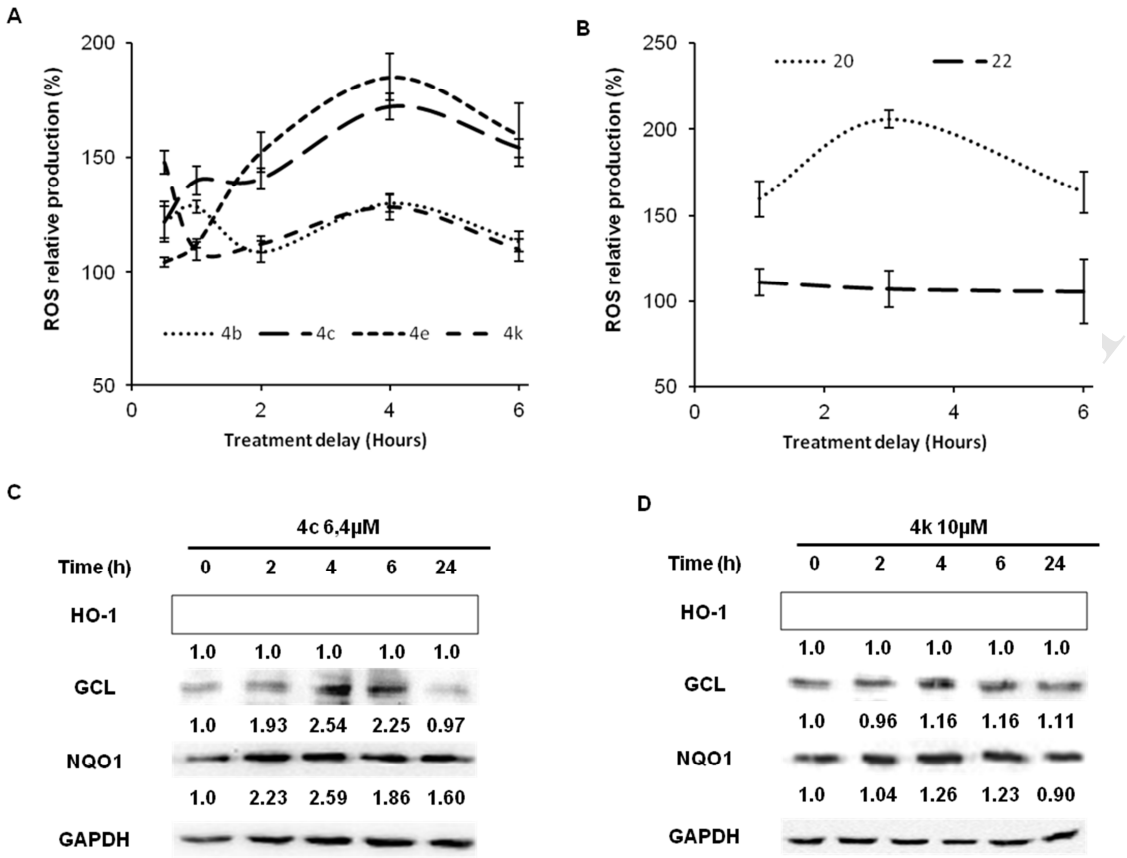

Fig. 4. Thiazolidin-4-one derivative treatment is associated with ROS production and modulation of antioxidant enzyme expression.

A and **B:** ROS production was calculated in HT29 treated cells with compound **4a, 4c, 4e** or **4k**, and compound **20** or **22** as described in the biological methods section. **C** and **D**: Western blotting was performed as described in the Biological methods section. Respective mouse or rabbit diluted antibodies against HO-1 (1: 1 000), NQO1 (1:1 000), GCL (1: 500) were used. GAPDH antibodies (1: 10 000) were used as an internal loading control Typical results obtained when HT29 cells were treated with compound **4c** and **4k**.

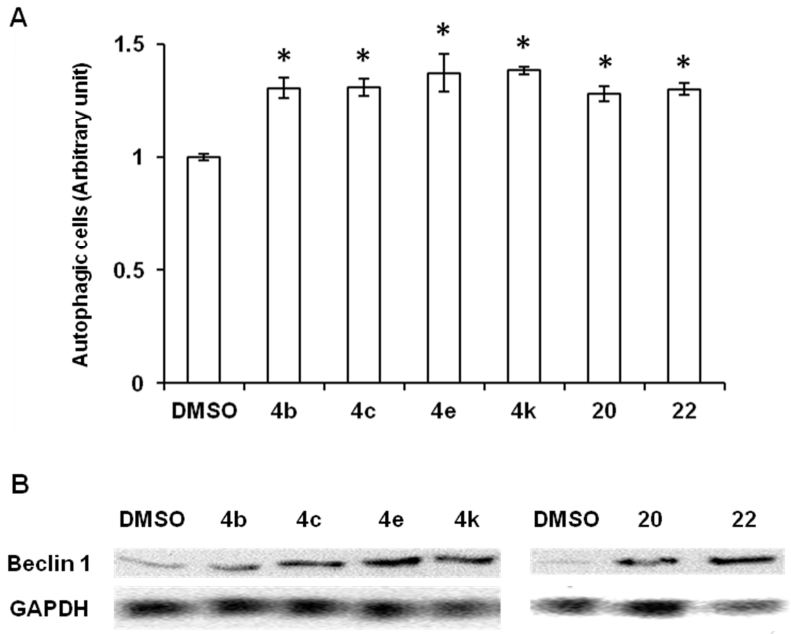

Fig. 5. Autophagy processes in HT29 exposure to thiazolidin-4-one derivatives.

A. autophagy process was quantified inHT29 cells exposed to each compound as described in the biological methods section.*, significant difference at Student t test ($P<0.05$) with respect to DMSO-treated cells.

B. Detection of beclin-1 expression during autophagosome formation by western blotting. The experiments were performed with rabbit antibody against human beclin-1 as described in the biological methods section. Typical results out of three independent experiments obtained with protein homogenates prepared from HT29 cells treated with each compound over two days. Mouse antibody against human GAPDH was used as sample loading.

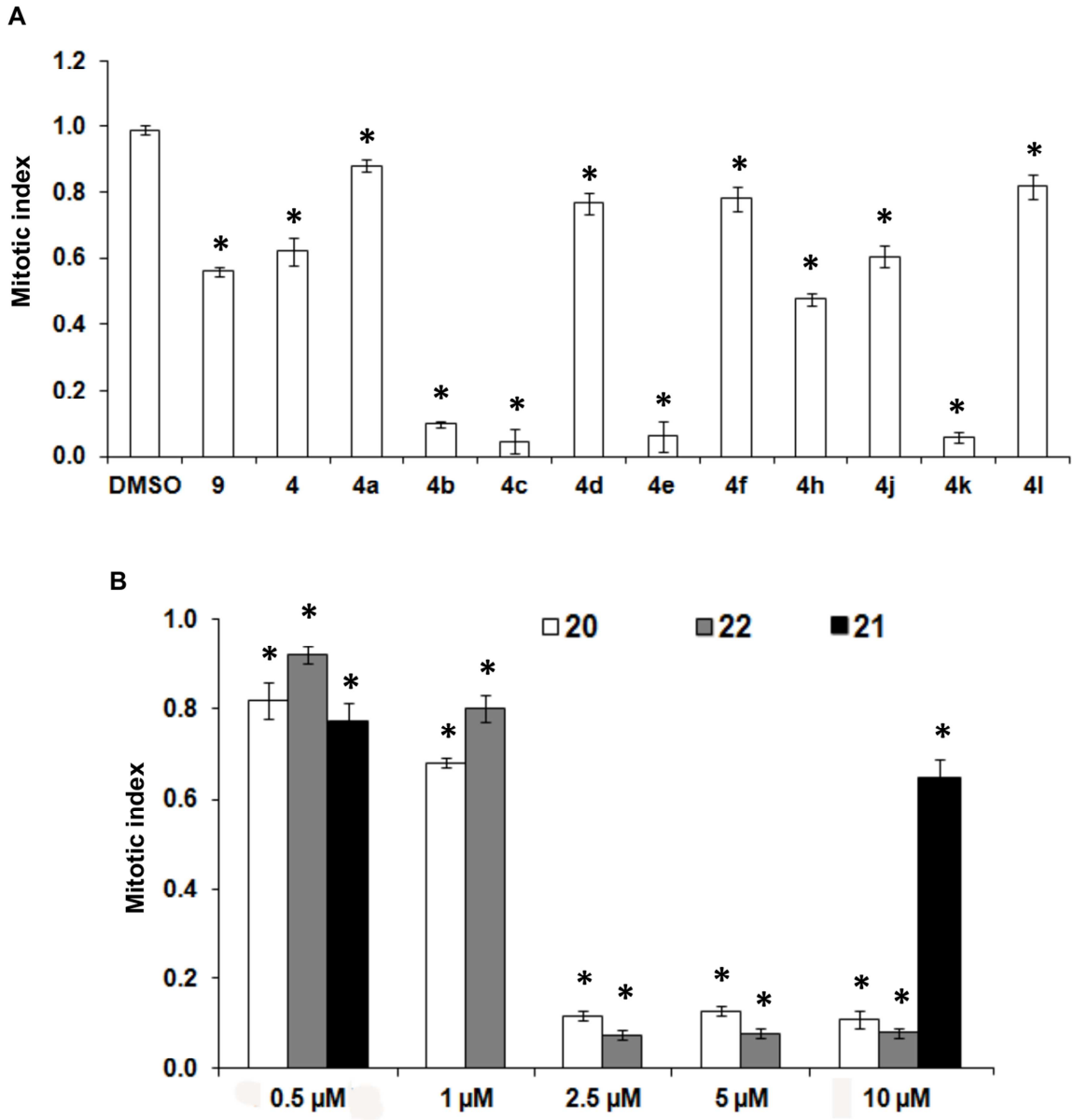
A
Mitotic index
1.2
1.0
0.8
0.6
0.4
0.2
0.0
DMSO
9
4
4a
4b
4c
4d
4e
4f
4h
4j
4k
4l
B
Mitotic index
1.0
0.8
0.6
0.4
0.2
0.0
20
22
21
0.5 μM
1 μM
2.5 μM
5 μM
10 μM

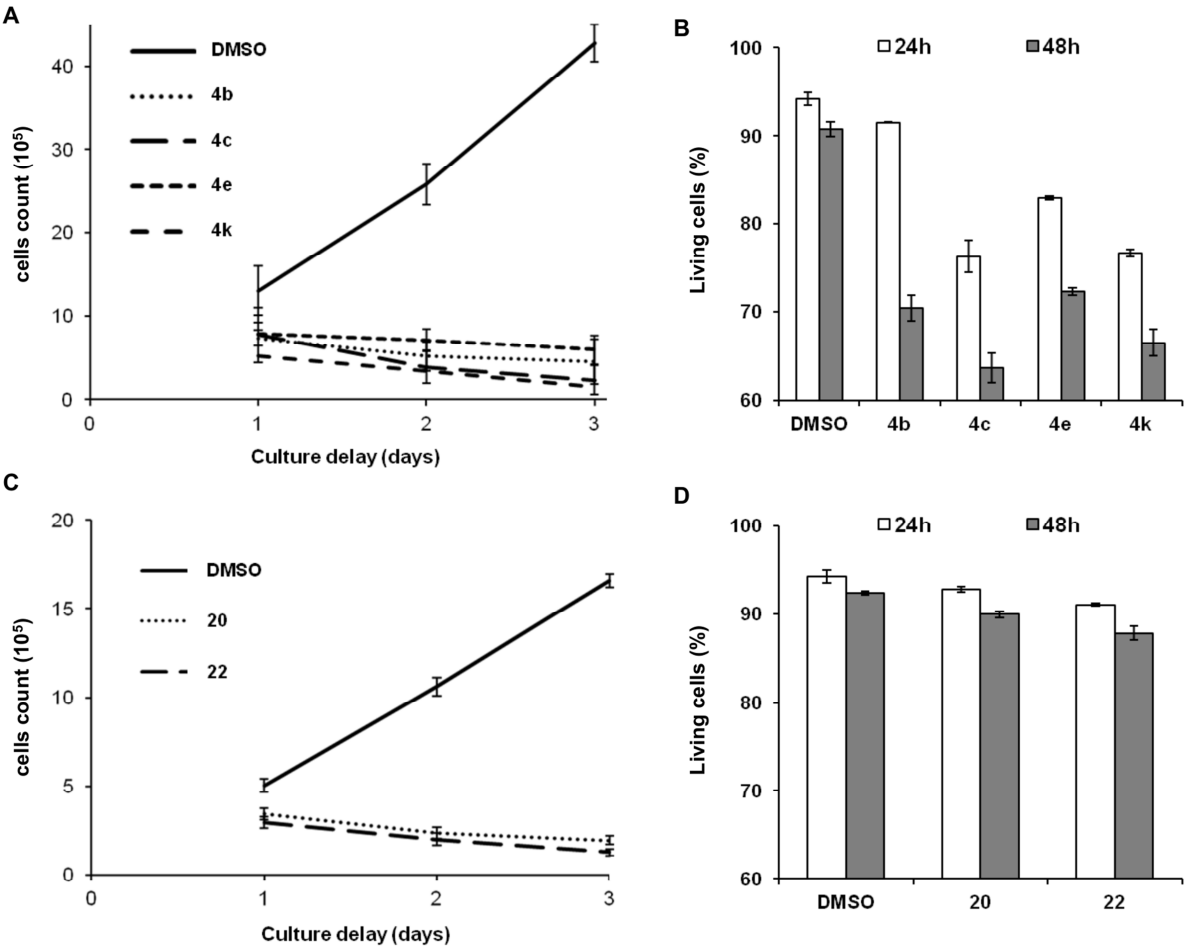
A
DMSO
4b
4c
4e
4k
cells count (10⁵)
Culture delay (days)
B
24h
48h
Living cells (%)
DMSO
4b
4c
4e
4k
C
DMSO
20
22
cells count (10⁵)
Culture delay (days)
D
24h
48h
Living cells (%)
DMSO
20
22

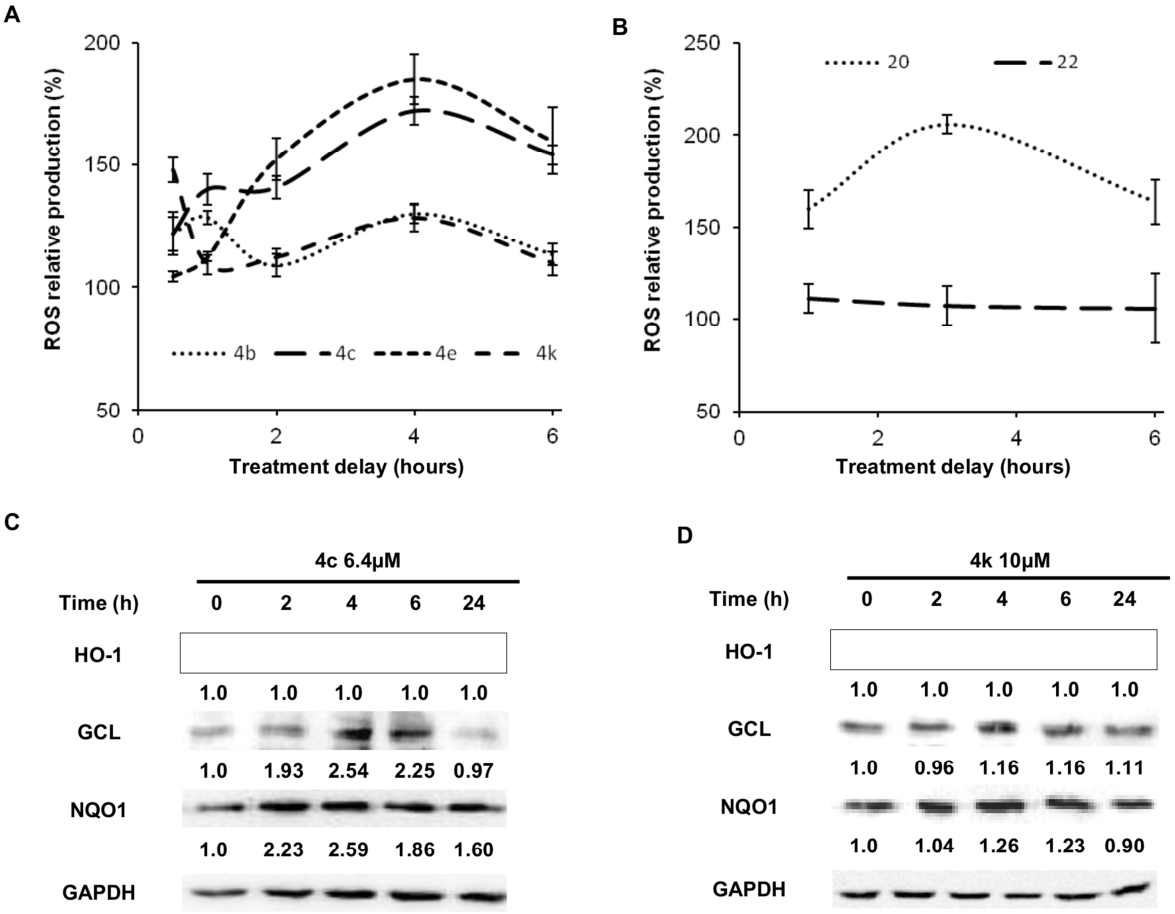
A
ROS relative production (%)
200
150
100
50
0
2
4
6
Treatment delay (hours)
4b
4c
4e
4k
B
ROS relative production (%)
250
200
150
100
50
0
2
4
6
Treatment delay (hours)
20
22
C
4c 6.4μM
Time (h)
0
2
4
6
24
HO-1
1.0 1.0 1.0 1.0 1.0
GCL
1.0 1.93 2.54 2.25 0.97
NQO1
1.0 2.23 2.59 1.86 1.60
GAPDH
D
4k 10μM
Time (h)
0
2
4
6
24
HO-1
1.0 1.0 1.0 1.0 1.0
GCL
1.0 0.96 1.16 1.16 1.11
NQO1
1.0 1.04 1.26 1.23 0.90
GAPDH

A

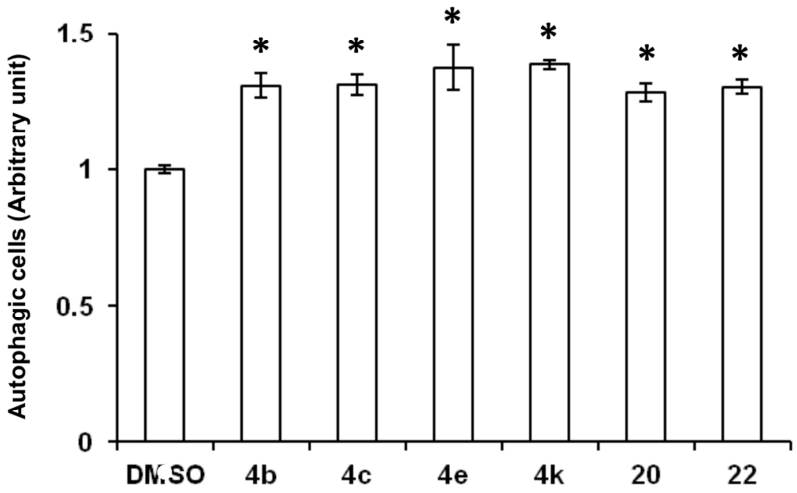

B

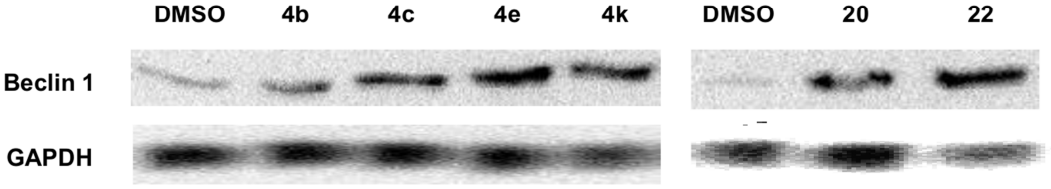

Highlights

- 35 Heteroaryliminothiazolidinones were synthesized.
- Their antiproliferative properties were investigated.
- Benzylidene moiety on 5-position of the thiazolidinone gave more potent compounds.
- Derivatives with a thiazolylimino moiety showed promising cytotoxicity.
- Accumulation in G2/M phase and in subG1 fraction was observed.

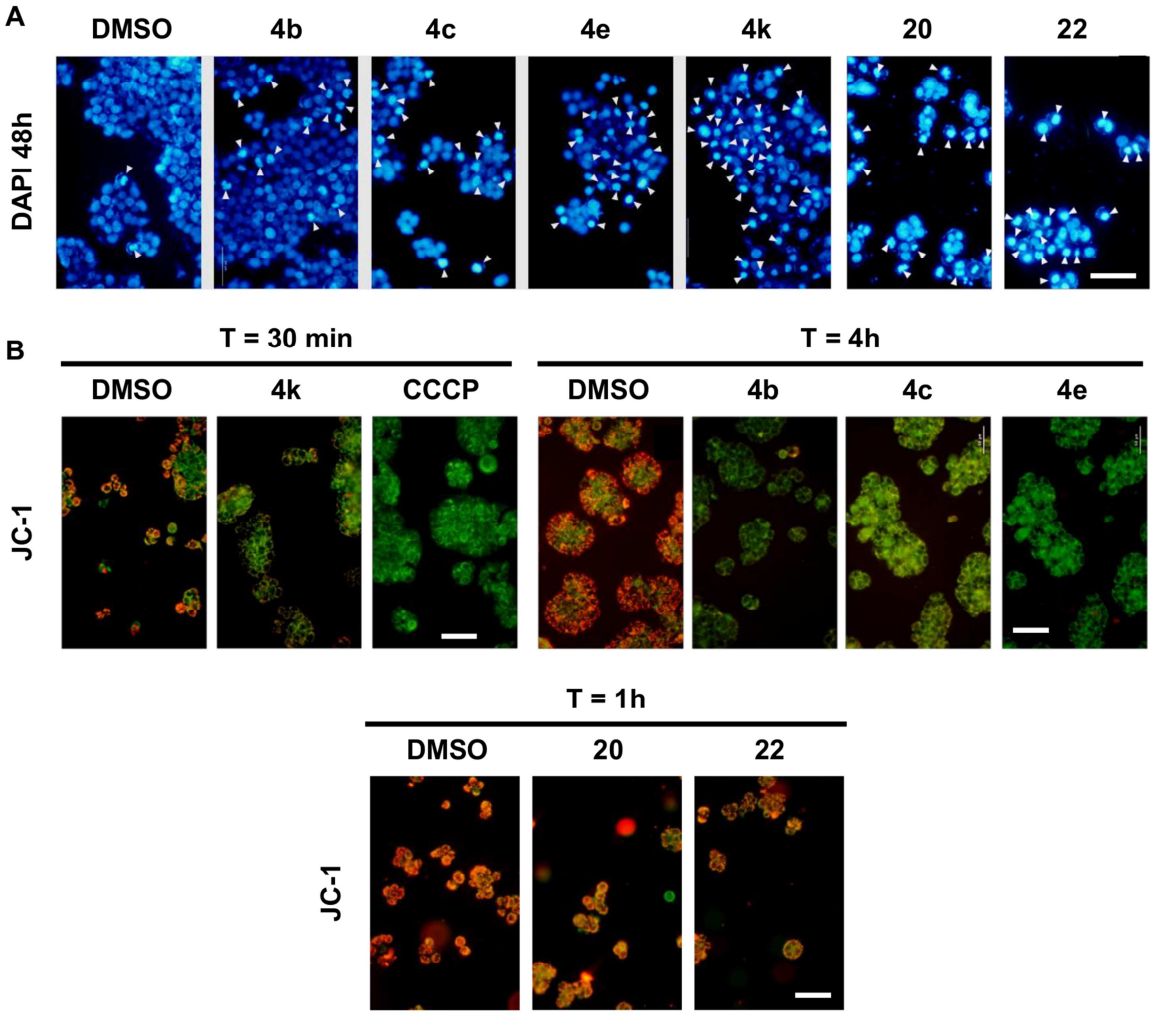

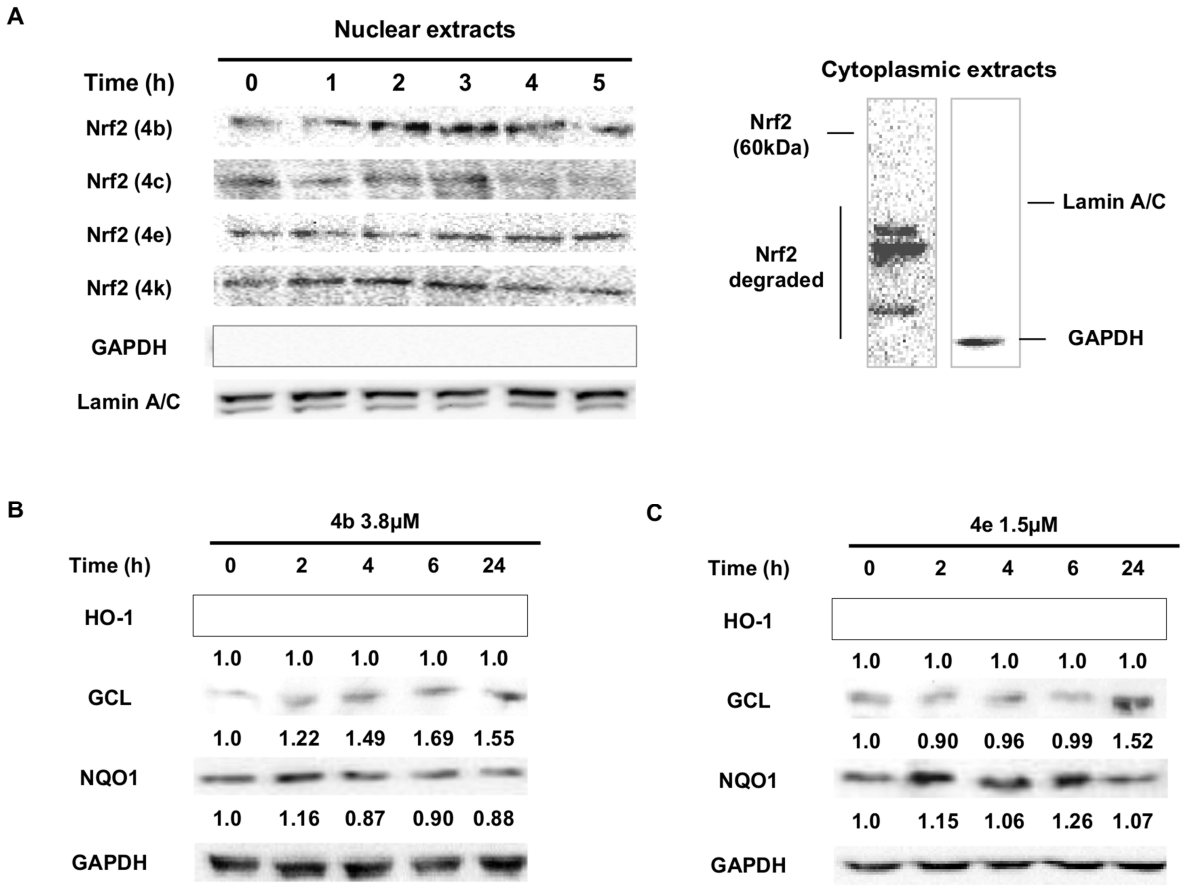

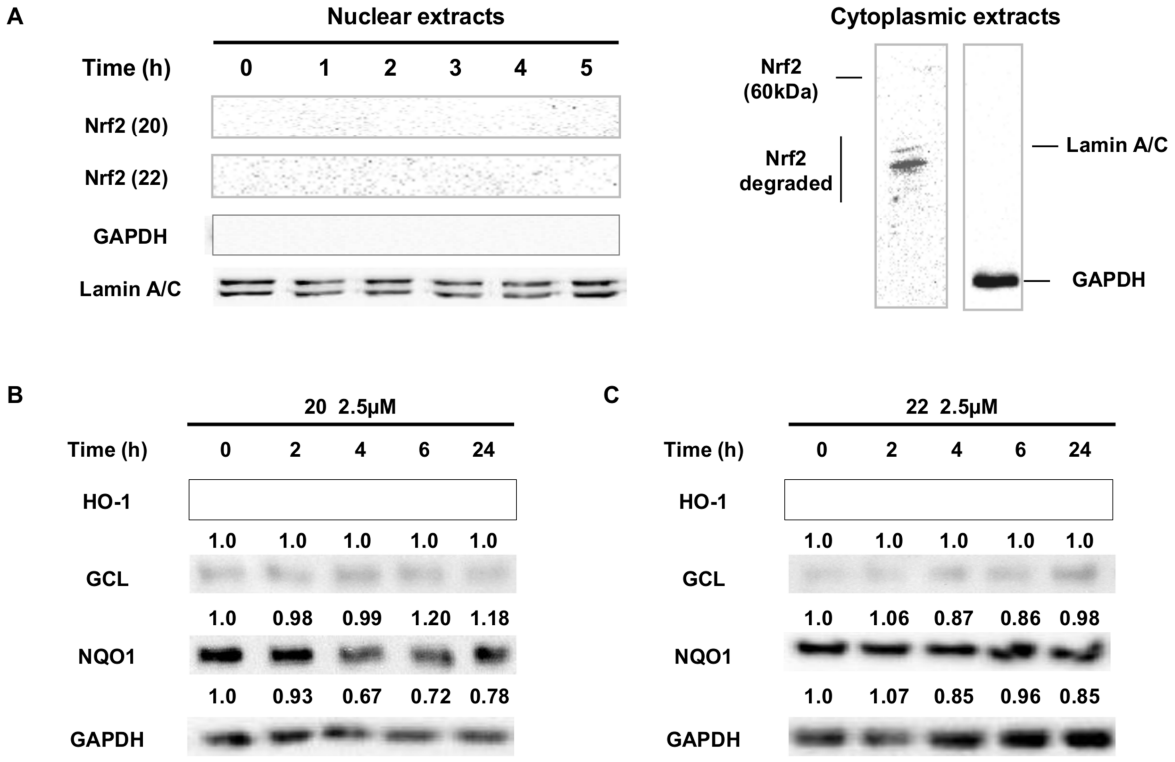

Supporting information

Synthesis and biological evaluation of novel 2-heteroarylimino-1,3-thiazolidin-4-ones as potential anti-tumor agents

Germain Revelant[1,a], Sophie Huber-Villaume[2,b], Sandrine Dunand[1], Gilbert Kirsch[1], Hervé Schohn[2,] ** and Stéphanie Hesse[1,] *

1. Université de Lorraine - UMR CNRS 7565 - Structure et Réactivité des Systèmes Moléculaires Complexes – Equipe 3 (HECRIN) - 1 Boulevard Arago, 57070 Metz Technopôle, France
2. Université de Lorraine - UMR CNRS 7565 - Structure et Réactivité des Systèmes Moléculaires Complexes – Equipe 5 (2MIC) – Campus Bridoux – rue du Général Delestraint – 57070 Metz Cedex, France

*Corresponding author: Tel.: +33 3 87 54 74 97. Fax: + 33 3 87 31 58 01.
** Corresponding author: Tel.: +33 3 87 37 84 09. Fax:+ 33 3 87 31 58 01
E-mail addresses: herve.schohn@univ-lorraine.fr (H. Schohn), stephanie.hesse@univ-lorraine.fr (S. Hesse)

Supporting Information S1.1

Synthesis of derivatives **4(a-l)** starting from **4**.

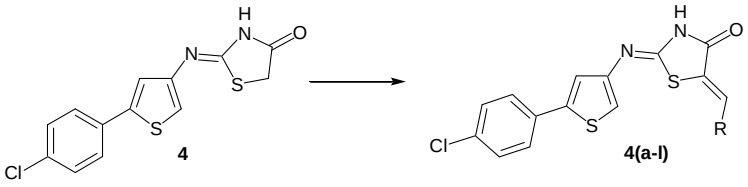

Reagents and conditions: RCHO, pyrrolidine, MeOH, reflux, 20h.

Compound	R	Yield (%)	Compound	R	Yield (%)
4a	Ph	56	**4g**	p-OH-Ph	76
4b	p-OMe-Ph	75	**4h**	2-naphtyl	89
4c	p-Me-Ph	69	**4i**	Hexyl	60
4d	p-Cl-Ph	71	**4j**	2-pyridinyl	76
4e	p-NMe_2-Ph	79	**4k**	3,4-diOMe-Ph	72
4f	p-Br-Ph	68	**4l**	p-F-Ph	54

Supporting Information S1.2

Synthesis of derivatives **12-17**.

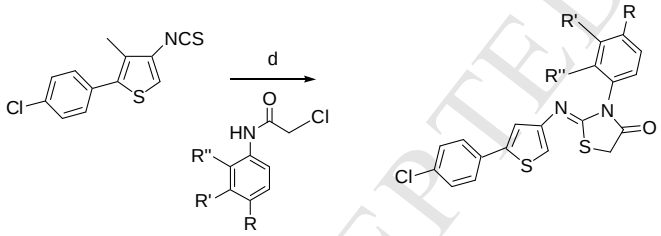

Reagents and conditions: (d) K_2CO_3, CH_3CN, 40°C.

Compound	R	R’	R’’	Yield (%)
12	Cl	H	H	71
13	H	H	H	83
14	Me	H	H	90
15	NMe_2	H	H	84
16	OMe	OMe	H	59
17	H	C_4H_4		92

Supporting Information S1.3

Synthesis of derivatives **20-24**.

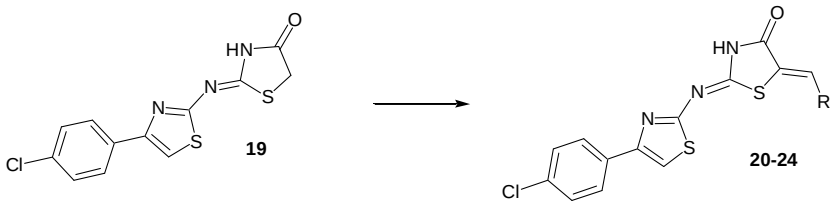

Reagents and conditions: RCHO, pyrrolidine, MeOH, reflux, 20h.

Compound	R	Yield (%)
20	p-NMe_2-Ph	86
21	p-Me-Ph	68
22	p-OMe-Ph	79
23	2-naphtyl	85
24	p-F-Ph	82

Supporting Information S2

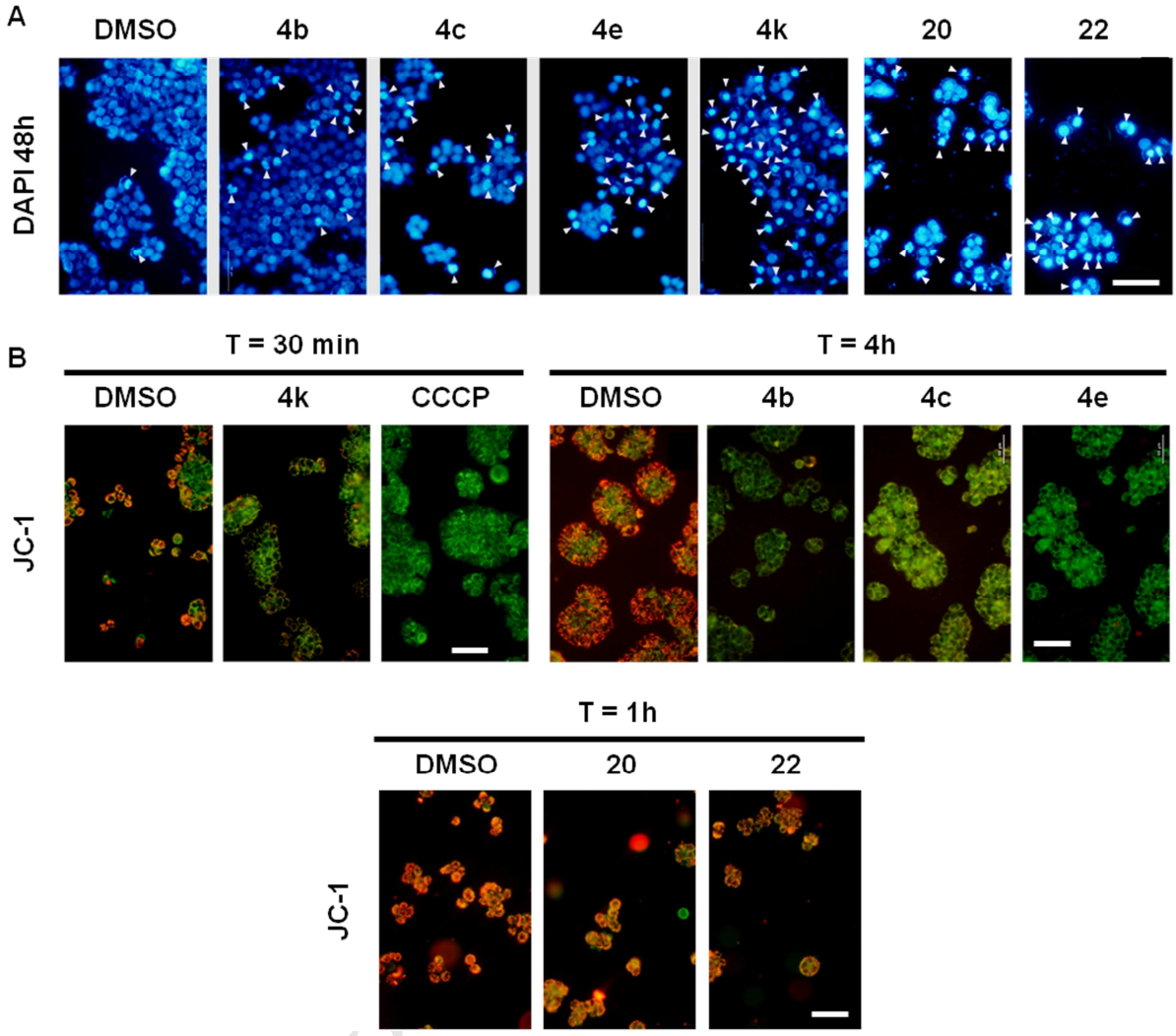

HT29 cell-living imaging after treatment with thiazolidinone derivatives

HT29 cells were treated in the presence of each compound for one day as described in the biological methods section and loaded with DAPI (**A**) or JC-1 (**B**) fluorescent probes. Nuclei with condensed chromatin (white arrow heads, in **A**) were observed when cells were treated with respective compound and loaded with DAPI probe. HT29 cells exposure to compound **4b**, **4c**, **4e** or **4k** was associated with the loss of Ψm as visualized by the absence of J-aggregates (orange/red) within the cells (typical results obtained after 30 min- and 4hours-treatment duration (**B**). CCCP (50 µM for 15 min) was used to dissipate Ψm as shown by the absence of J-aggregates as compared to the results obtained after cell exposure to DMSO (molecule vehicle). In contrast, no Ψm dissipation was observed after HT29 cells exposure to compound **20** or **22** at any time (typical results obtained from HT29 cells exposed 1 hour to each compound and loaded with JC-1 probe).(Bars = 50 µm, in A and B)

Supporting Information S3

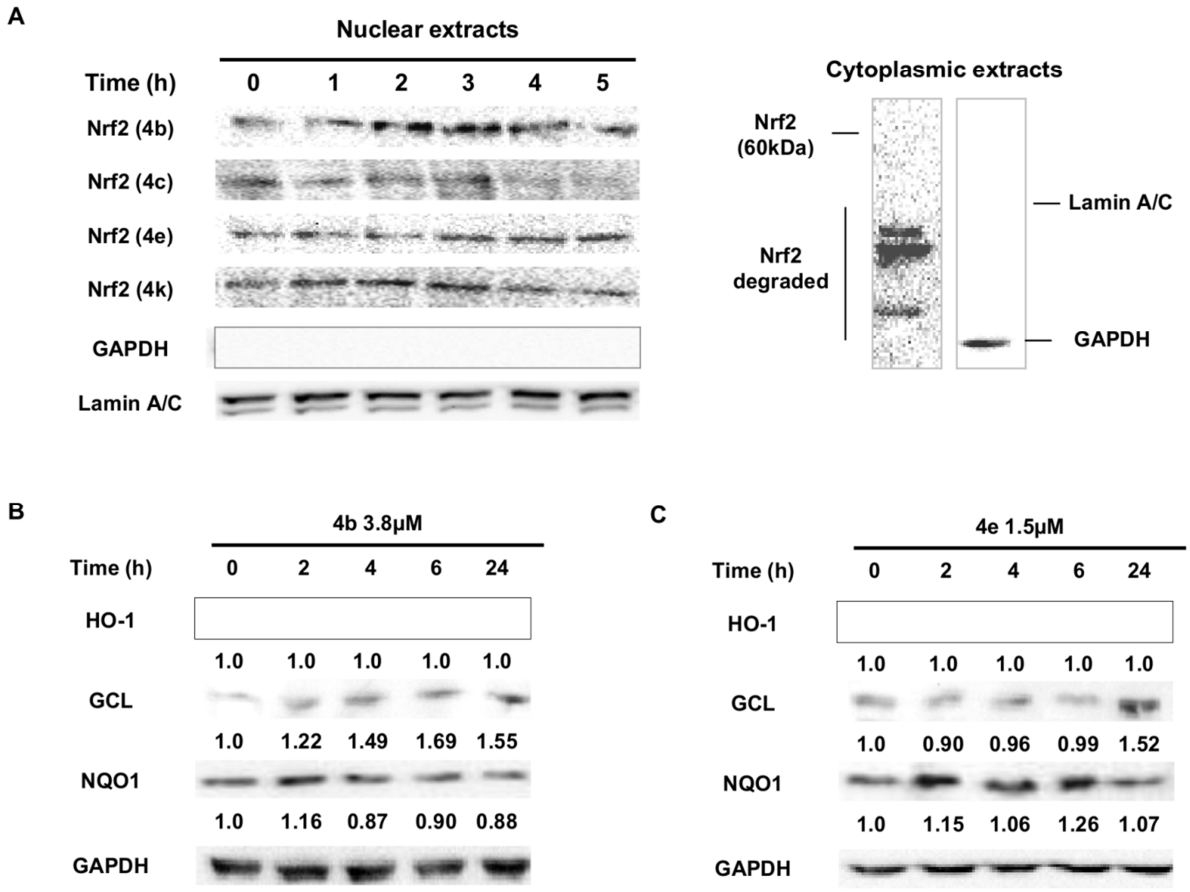

Modulation of Nrf2/Keap1 signaling and antioxidant enzyme expression

A and **B**. HT29 cells treated with **4b**, **4c**, **4e** or **4k.**. Nuclei and cell homogenates were prepared as described in the biological methods section. Respective mouse or rabbit diluted antibodies against Nrf2 (1: 500), HO-1 (1: 1 000), NQO1 (1:1 000), GCL (1: 500) were used. Each blot was stripped and used to detect human GAPDH (1: 10 000) using the same protocol. Bands were quantified and normalized to GAPDH content. The ratio, level of protein of interest *versus* GAPDH content, in DMSO-treated cells was considered as 1.00. Results shown are representative of one out of three independent experiments. Typical results obtained when HT29 cells were treated with compound **4b** and **4e**.

Supporting Information S4

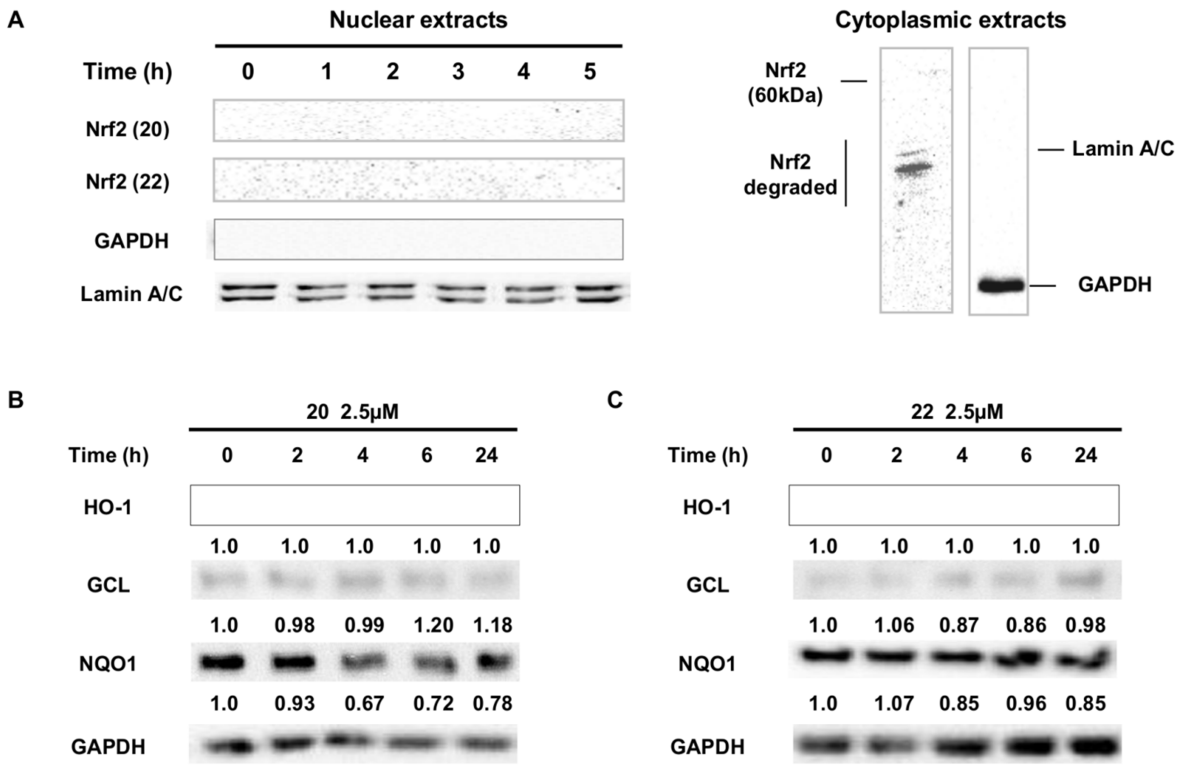

Modulation of Nrf2/Keap1 signaling and antioxidant enzyme expression

A and **B**. HT29 cells treated with **20** or **22**. Nuclei and cell homogenates were prepared as described in the biological methods section. Respective mouse or rabbit diluted antibodies against Nrf2 (1: 500), HO-1 (1: 1 000), NQO1 (1:1 000), GCL (1: 500) were used. Each blot was stripped and used to detect human GAPDH (1: 10 000) using the same protocol. Bands were quantified and normalized to GAPDH content. The ratio, level of protein of interest *versus* GAPDH content, in DMSO-treated cells was considered as 1.00. Results shown are representative of one out of three independent experiments. Typical results obtained when HT29 cells were treated with compound **20** and **22**.